Chloroplast Photooxidation-Induced Transcriptome Reprogramming in Arabidopsis *immutans* White Leaf Sectors[1][W][OA]

Maneesha R. Aluru, Jaroslaw Zola, Andrew Foudree, and Steven R. Rodermel*

Department of Genetics, Development, and Cell Biology (M.R.A., A.F., S.R.R.) and Department of Electrical and Computer Engineering (J.Z.), Iowa State University, Ames, Iowa 50011

Arabidopsis (*Arabidopsis thaliana*) *immutans* (*im*) has green and white sectoring due to the action of a nuclear recessive gene, *IMMUTANS*. The green sectors contain normal-appearing chloroplasts, whereas the white sectors contain abnormal chloroplasts that lack colored carotenoids due to a defect in phytoene desaturase activity. Previous biochemical and molecular characterizations of the green leaf sectors revealed alterations suggestive of a source-sink relationship between the green and white sectors of *im*. In this study, we use an Affymetrix ATH1 oligoarray to further explore the nature of sink metabolism in *im* white tissues. We show that lack of colored carotenoids in the *im* white tissues elicits a differential response from a large number of genes involved in various cellular processes and stress responses. Gene expression patterns correlate with the repression of photosynthesis and photosynthesis-related processes in *im* white tissues, with an induction of Suc catabolism and transport, and with mitochondrial electron transport and fermentation. These results suggest that energy is derived via aerobic and anaerobic metabolism of imported sugar in *im* white tissues for growth and development. We also show that oxidative stress responses are largely induced in *im* white tissues; however, *im* green sectors develop additional energy-dissipating mechanisms that perhaps allow for the formation of green sectors. Furthermore, a comparison of the transcriptomes of *im* white and norflurazon-treated white leaf tissues reveals global as well as tissue-specific responses to photooxidation. We conclude that the differences in the mechanism of phytoene desaturase inhibition play an important role in differentiating these two white tissues.

Green-white variegation in the Arabidopsis (*Arabidopsis thaliana*) *immutans* (*im*) mutant is induced by a nuclear recessive gene, *IMMUTANS* (*IM*). The green sectors contain cells with morphologically normal chloroplasts, whereas plastids in cells of the white sectors lack pigments and organized lamellar structures (Wetzel et al., 1994). The extent of white sector formation in *im* is dependent upon the illumination conditions during growth: increased light intensity causes enhanced white sector formation (nearly all-white plants), while nearly all-green plants are produced by growth under low-light conditions (for review, see Aluru et al., 2006).

Early biochemical experiments showed that white sectors of *im* accumulate phytoene, indicating that the phytoene desaturase (PDS) step of carotenogenesis is blocked in the mutant (Wetzel et al., 1994). Cloning of *IM* by map-based and T-DNA-tagging procedures revealed that the gene product is homologous to alternative oxidase (AOX) of mitochondrial inner membranes (Carol et al., 1999; Wu et al., 1999). In fact, it is now well established that IM, like AOX, serves as a terminal (quinol) oxidase in thylakoid membranes, where it accepts electrons from plastoquinol and transfers them to molecular oxygen to generate water (Cournac et al., 2000; Carol and Kuntz, 2001; Joet et al., 2002; Aluru et al., 2006; Rosso et al., 2006). IM is expressed ubiquitously in Arabidopsis and has been suggested to play a global role in plastid metabolism (Aluru et al., 2001; Yu et al., 2007).

One process where IM acts as a terminal oxidase is during the desaturation reactions of carotenogenesis: electrons from phytoene are transferred to the plastoquinone pool via PDS and then to molecular oxygen via IM (Josse et al., 2000). Accordingly, it has been hypothesized that a lack of IM would lead to overreduction of the plastoquinone pool and to an accumulation of phytoene, preventing the formation of colored carotenoids (Joet et al., 2002; Aluru et al., 2006; Rosso et al., 2006). Since colored carotenoids protect chloroplasts against reactive oxygen species (ROS)-induced photooxidation by quenching triplet chlorophyll and singlet oxygen (Demmig-Adams et al., 1996), this suggests that the plastids in *im* white (*im*W) sectors are photooxidized. This notion is consistent with results from plants treated with norflurazon (NF), which have photobleached plastids and an

[1] This work was supported by the U.S. Department of Energy (Energy Biosciences grant no. DE–FG02–94ER20147 to S.R.R.).

* Corresponding author; e-mail rodermel@iastate.edu.

The author responsible for distribution of materials integral to the findings presented in this article in accordance with the policy described in the Instructions for Authors (www.plantphysiol.org) is: Steven R. Rodermel (rodermel@iastate.edu).

[W] The online version of this article contains Web-only data.

[OA] Open Access articles can be viewed online without a subscription.

www.plantphysiol.org/cgi/doi/10.1104/pp.109.135780

albino phenotype due to the inhibition of PDS activity (Tonkyn et al., 1992; Brietenbach et al., 2001; Dalla Vecchia et al., 2001).

Green and white cells of *im* have the same genotype (*im*/*im*), and an important question of our research is, how do the green sectors form? To gain insight into this question, we have characterized *im* green (*im*G) sectors by morphological, biochemical, and global gene expression studies (Aluru et al., 2001, 2007). These studies showed that compared with wild-type Arabidopsis leaves, *im*G sectors have anatomical and molecular alterations indicative of a high-light-acclimated plant: mesophyll cell sizes are enlarged, and photoprotective genes, such as those involved in oxidative stress and phenylpropanoid and flavonoid biosynthesis, are significantly induced (Aluru et al., 2001, 2007). The *im*G sectors also have enhanced photosynthetic rates and increased Rubisco and Suc-P synthase activities. These increases result in an increase in starch and Suc accumulation. We hypothesized that these alterations are due to source-sink interactions between the green and white sectors that might serve to optimize plant growth. In support of this hypothesis, *im*W sectors accumulate low levels of Suc and have increased acid invertase activities compared with *im*G sectors, suggesting that there might be a Suc gradient between these two tissue types, with Suc being transported from green to white in response to sink demand. Therefore, one question motivating the current studies is the nature of "sink metabolism" in the white leaf tissues of *im*.

As a first approach to address this question, we performed global transcript profiling of white *im* leaf sectors using the 22K ATH1 Arabidopsis array. To our knowledge, a comprehensive transcriptome analysis of the metabolic adaptations occurring in mature white leaf tissues has not yet been reported. In fact, only one other study detailing genome-wide changes relating to metabolism and transport in sink tissues has been published (Deeken et al., 2006). These studies were performed in Arabidopsis tumors and showed that tumors import sugars and amino acids from uninfected tissues and generate energy mainly by anaerobic metabolism via fermentation for rapid growth and development. Our studies show the utilization of similar strategies by *im*W leaf sectors, but our data further suggest that *im*W tissues use a combination of various energy-producing mechanisms for growth and development.

To gain further insight into the molecular phenotype of *im*W tissues, we compared the transcriptomes of *im*W and *im*G and the transcriptomes of *im*W and NF-treated white Arabidopsis leaf tissues. Because the two white tissue types have many morphological, biochemical, and molecular similarities (Brown et al., 2001; Rodermel, 2001; Gray et al., 2002; Sullivan and Gray, 2002; Surpin et al., 2002), our initial hypothesis was that they would have similar, if not identical, molecular phenotypes. Surprisingly, we found that there are distinct as well as shared gene expression patterns between NF-treated and *im*W tissues.

RESULTS

Transcript Profiling of *im*W Leaf Sectors

As a first approach to characterize *im*W sectors, we performed global transcript profiling using the Affymetrix ATH1 oligoarray containing approximately 22,500 genes. The experiments were conducted in triplicate (three different biological replicates) using total cell RNAs from *im*W sectors of rosette leaves; wild-type leaves of similar developmental stages served as controls. To assess the quality of the microarray data, scatterplots were generated to compare the expression values of all chips in a pairwise fashion (e.g. chip *im*-1 versus chip WT-1). Linear relationships were observed in the different comparisons; the three biological replicates displayed an especially strong linearity (e.g. chips *im*-1, *im*-2, and *im*-3; Supplemental Fig. S1).

We used the software packages R and Bioconductor and Microarray Suite 5.0 to extract expression values from GeneChips and to normalize the raw probe values (Bolstad et al., 2003; Irizarray et al., 2003; Gentleman et al., 2005). To avoid the occurrence of false positives, we further applied a 2-fold cutoff filter and chose genes/ATH1 probe sets with an adjusted *P* value of 0.05 or less. Figure 1 shows the distribution of probe sets/genes on the basis of fold change in transcript abundance in the *im*W compared with the wild-type samples. The transcripts of most genes varied in abundance by less than 2-fold (similar to the wild type), but those of 1,434 probe sets changed in abundance by 2-fold or more. Of the 1,434 "differentially regulated" genes, 687 were repressed and 747 were induced. These results were confirmed by quantitative real-time reverse transcription (RT)-PCR analyses of select genes (Fig. 2).

Functional Classification of *im*-Responsive Genes

To ascertain the biological significance of the microarray data, the 1,434 differentially regulated genes were placed into functional groups using the Arabidopsis Munich Information Center for Protein Sequences (MIPS) classification scheme (http://mips.gsf.de/proj/thal/db/) and gene ontology searches (http://www.arabidopsis.org/; see Supplemental Table S1 for a complete list). Figure 3 summarizes the data and shows that all classes of genes are represented; most classes contain induced genes as well as repressed genes. However, it is notable that nearly all of the differentially regulated genes for photosynthesis are repressed in *im*W, while nearly all of those for electron transport, secondary metabolism, and plant development are induced.

Major Metabolic Pathways Affected in *im*W Tissues

To obtain a better understanding of the functional significance of the 1,434 differentially regulated genes,

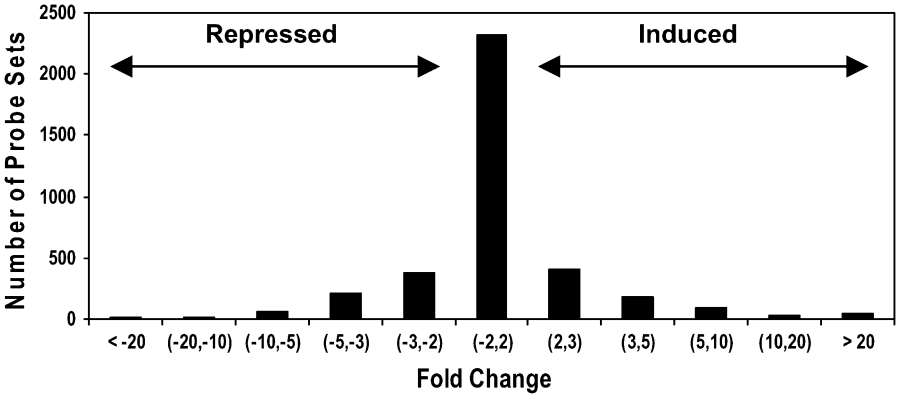

Figure 1. Distribution of transcript changes in *im*W leaf sectors compared with the wild type. The distribution includes those genes having a 2-fold or more increase (Induced) or decrease (Repressed) in normalized signal intensities and an adjusted *P* value of 0.05 or less.

we focused on those that play a role in well-characterized biochemical pathways of photosynthetic cells using MapMan, a bioinformatics tool commonly used for microarray data visualization (Thimm et al., 2004); we have previously used this tool for transcriptomics analysis of *im*G sectors (Aluru et al., 2007). Figure 4 shows that *im*-responsive genes are distributed among all metabolic pathways but that some have more differentially regulated genes than others. These pathways are discussed below.

Photosynthesis

Consistent with the data in Figure 3, one of the most striking alterations in the transcriptome of *im*W tissues involves the repression of genes for proteins that function in photosynthesis. Many of the genes (approximately 47 of 120) that mediate the light reactions of photosynthesis are repressed in *im*W. An exception is cytochrome c_6 (AT5G45040), which transfers electrons to PSI and is thought to prevent overoxidation of PSI at its lumenal side and overreduction at its stromal side (Howe et al., 2006). Genes encoding key enzymes of the Calvin cycle and photorespiration are also repressed in *im*W. These include phosphoglycerate kinase (AT1G56190), Fru-bisP aldolase (AT2G21330) Fru-1,6-bisphosphatase (AT3G54050), sedoheptulose-1,7-bisphosphatase (AT3G55800), phosphoribulokinase (AT1G32060), phosphoglycolate phosphatase (AT5G36700), Gly cleavage system H protein (AT1G32470), Gly cleavage system H protein 1 (AT2G35370), and carbonic anhydrases (AT3G52720, AT4G33580, and *CA1*). Furthermore, there is a repression of genes for enzymes that mediate key steps in the biosynthesis of photosynthetic pigments, such as chlorophyll (*PORB* and *PORC*; 5- to 10-fold) and carotenoids (*PSY* and *GGPS*; 3- and 2-fold, respectively); PORB and PORC are crucial for the photoconversion of protochlorophyllide to chlorophyllide, which is then converted to chlorophyll (Masuda et al., 2003). Likewise, PSY is the key regulatory step of carotenogenesis in plastids (Hirschberg, 2001). An exception to the repression of key pigment genes is the induction of *FLU*, which is a negative regulator of *HEMA1* (Meskauskiene et al., 2001). HEMA1 catalyzes the rate-limiting step in tetrapyrrole biosynthesis; thus, the induction of *FLU* might be indicative of a decrease in HEMA1 activity.

Taken together, the repression of genes involved in the light and dark reactions of photosynthesis, photorespiration, and pigment biosynthesis is consistent with the fact that *im*W tissues do not undergo photosynthesis. It is worth pointing out that down-regulation of *rbcS* (for Rubisco small subunit) is often used as diagnostic of retrograde signaling (repression in the presence of NF; Nott et al., 2006). However, Figure 4 shows

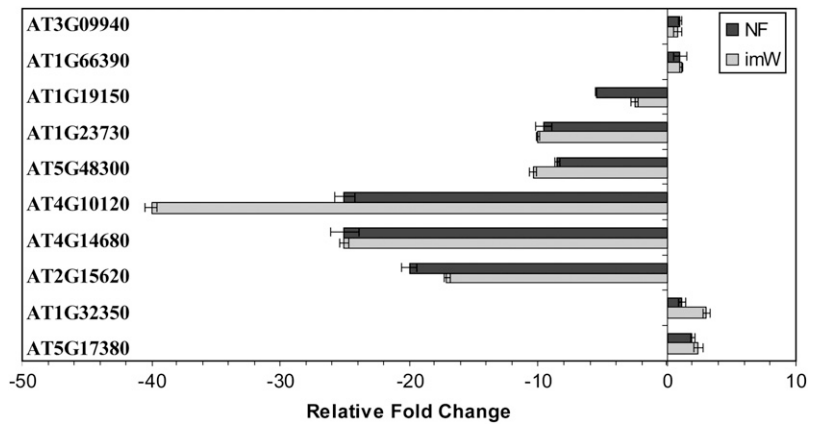

Figure 2. Quantitative real-time RT-PCR. The expression levels of genes from *im*W and NF-treated tissues were measured by real-time RT-PCR. Fold change values were calculated according to Hewezi et al. (2008) and represent changes in the two white tissues relative to the wild type. The data were normalized using *ACT12* accumulation as a control and are averages ± SD of three replicates.

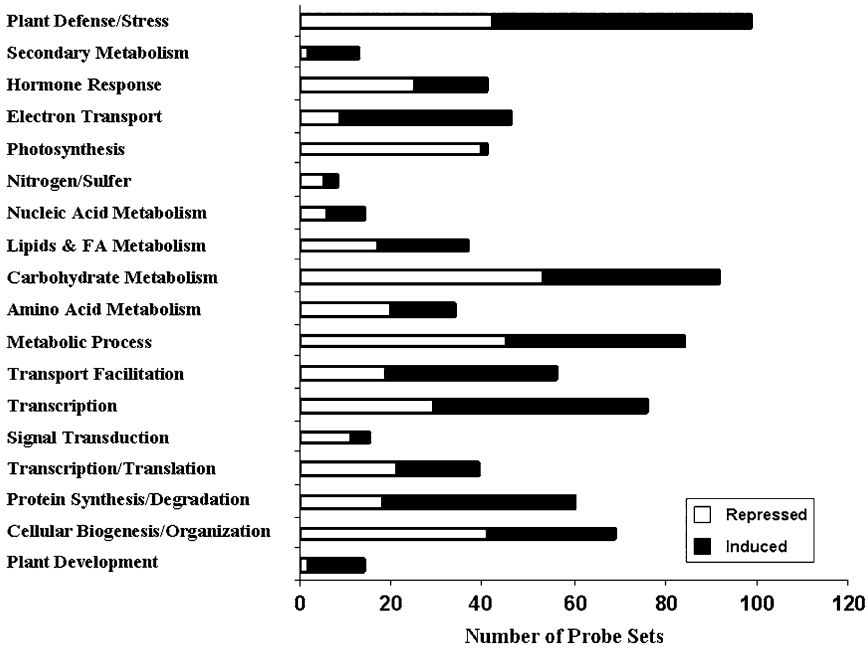

Figure 3. Functional classes of genes. The 1,434 *im*-responsive genes were assigned to functional classes based on the Arabidopsis MIPS classification scheme (http://mips.gsf.de/proj/thal/db/) and gene ontology searches (http://www.arabidopsis.org/). A detailed classification of genes is given in Supplemental Table S1.

that *rbcS* is not differentially regulated in white tissues. This is consistent with previous *rbcS* transcript accumulation data in Arabidopsis microarrays (Strand et al., 2003) and lends confirmation to the reliability of our microarray data.

Carbohydrate Metabolism

In accord with the general inhibition of photosynthesis in the *im*W tissues, our data show that genes for key enzymes of starch biosynthesis and degradation and of Suc biosynthesis are also strongly repressed in *im*W. Among these are ADP-Glc pyrophosphorylase small subunit (*ADG1*; 4-fold), starch synthase 1 (AT5G24300), starch-branching enzyme III (AT2G36390), starch-debranching enzymes (AT4G09020, AT1G03310, and AT2G36390), *AMY3*, β-amylase (AT4G00490), 4-α-glucanotransferase (AT5G64860), and Suc-P synthase (25-fold). These results are consistent with previous results from our laboratory showing that *im*W sectors do not accumulate starch and have low levels of Suc (Aluru et al., 2007). Exceptions to this general repression include genes for β-amylases (*BAM1* and *BAM9*), which are induced. β-Amylases were also found to be induced in the white leaf sectors of the barley (*Hordeum vulgare*) mutant *albostrians* (Hess et al., 1998).

In stark contrast to the repression of the Suc biosynthesis gene, our data show a strong induction of several genes for proteins involved in Suc degradation, such as a Suc synthase (AT5G20830), fructokinases (AT5G51830, AT3G54090, and AT1G69200), and invertase(s), including neutral (AT3G06500 and AT1G35580), vacuolar (*BFRUCT4*), and a cell wall invertase (*BFRUCT1*; 4-fold). Expression of the gene for a plastid-localized Glc-6-P/phosphate transporter (*GPT2*; 15-fold) and several sugar transporters (*STP1*; AT5G26340, AT2G43330, AT1G77210, and AT5G27350) is also strongly induced in *im*W tissues (Supplemental Table S1). Suc synthase, fructokinases, and invertases are major enzymes that metabolize imported Suc in sink tissues and play crucial roles in sink metabolism (Roitsch, 1999; Pego and Smeekens, 2000). Thus, the induction of these genes and genes mediating sugar transport further supports the notion of a source-sink relationship between green and white *im* leaf sectors and that *im*W tissues act as sinks of imported carbohydrate, primarily Suc.

Energy Production

Glycolysis. Genes that encode enzymes for the initial and committed steps of the glycolytic pathway (for review, see Plaxton, 1996) are repressed in *im*W. These include two phosphoglucomutases (AT1G70730 and AT1G70820), two phosphofructokinase family proteins (AT5G56630 and AT2G22480), and a pyruvate kinase (AT5G08570). Transcription of phospho*enol*pyruvate (PEP) carboxylases (PPC1 and PPC2) and PEP carboxy kinase involved in the conversion of PEP to oxaloacetate (OAA) is also repressed in *im*W, suggesting that carbon from the breakdown of Glc/Fru does not enter the tricarboxylic acid (TCA) cycle through the PEP carboxylase reaction. On the other hand, a member of the pyruvate kinase family (AT3G49160) is induced in *im*W.

Fermentation. Genes for enzymes involved in fermentation, including those for pyruvate decarboxylase (AT5G17380), alcohol dehydrogenase (*ADH1*; 11-fold), and an aldehyde dehydrogenase (AT1G54100; 10-fold), are significantly induced in *im*W tissues (for review, see Plaxton, 1996).

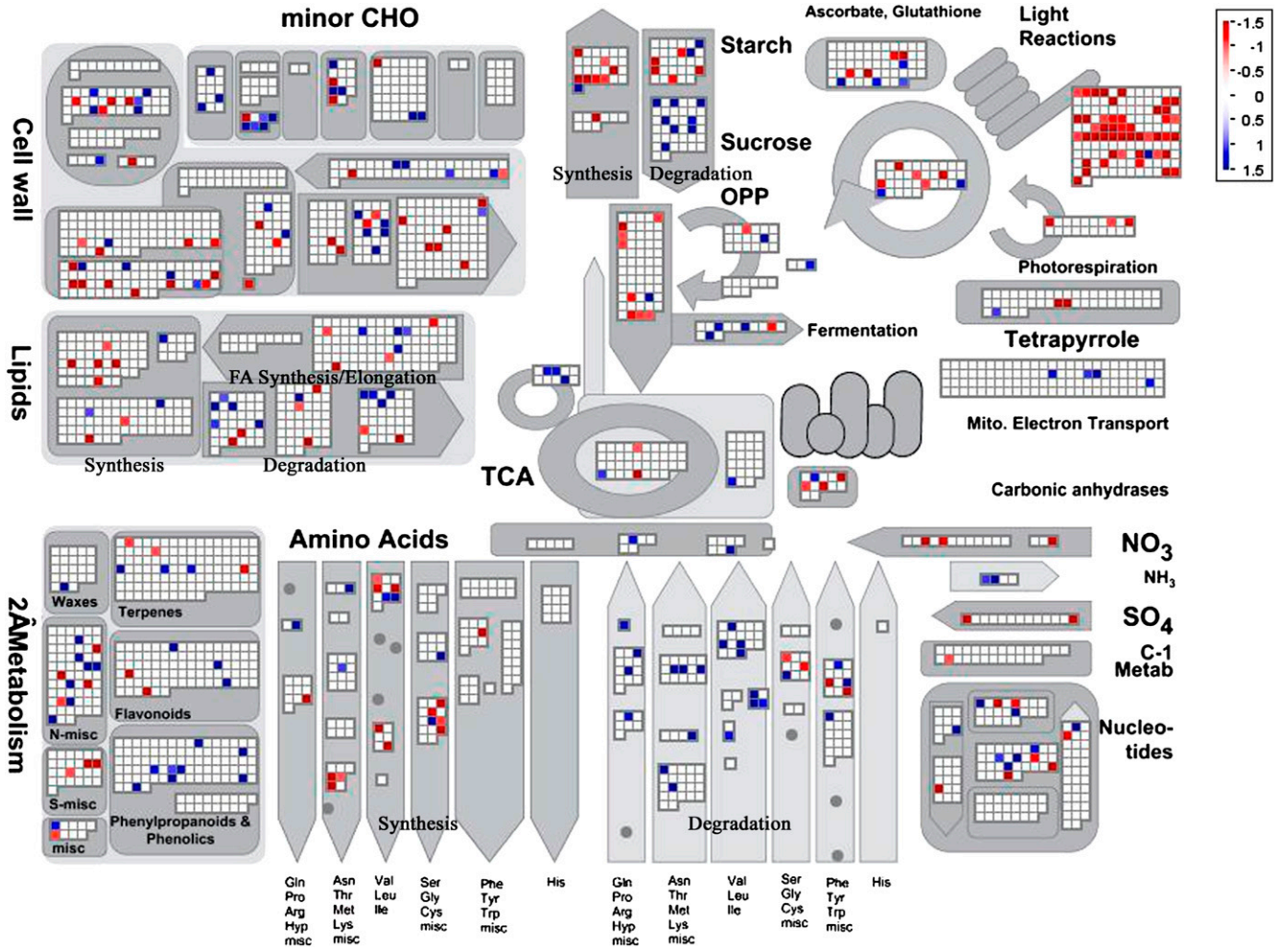

Figure 4. MapMan display of transcript profiling data. MapMan software (Thimm et al., 2004) was used to visualize changes in transcript abundance of the differentially regulated genes associated with major metabolic pathways from *im*W tissues. Induced genes are indicated in blue, and repressed genes are shown in red. White squares represent genes whose expression is unaltered versus the wild type. CHO, Carbohydrate.

Oxidative Pentose-P Pathway. Although only a few genes for enzymes of the oxidative pentose-P pathway are significantly altered in *im*W, transcription of two of the key enzymes of the pathway, Glc-6-P 1-dehydrogenase (AT1G09420; 3.8-fold) and 6-phosphogluconolactonase (AT1G13700; 3-fold; Kruger and von Schaewen, 2003) as well as a nonphotosynthetic tissue-specific ferredoxin are significantly induced. As expected, a plastidic Glc-6-P dehydrogenase (*G6PD/APG1*), which is expressed mostly in developing organs but is absent in nonphotosynthetic tissues (Kruger and von Schaewen, 2003), is repressed in the *im*W tissues.

TCA Cycle. The expression of most of the genes coding for enzymes of the TCA cycle (for review, see Fernie et al., 2004) is not significantly altered in *im*W tissues. Exceptions to this include repression of a fumarase (AT2G47510; 3-fold) and induction of succinate dehydrogenase (AT5G66760) and a cytosolic ATP-citrate synthase lyase (AT1G09430) that converts citrate to OAA.

Mitochondrial Electron Transport. Only a few genes for proteins of mitochondrial electron transport (for review, see Fernie et al., 2004) are significantly altered in *im*W. These include genes for proteins associated with complex II and complex IV and the alternative electron transport pathway, such as an electron transfer ubiquinone oxidoreductase (AT2G43400), succinate dehydrogenase (AT5G66760), cytochrome *c* oxidase assembly protein (AT1G53030), and alternative oxidases (*AOX1A* and *AOX1D*; 2- and 13-fold respectively). All of these genes are induced. Accompanying these increases, expression levels of mitochondrial metabolite transport genes (AT3G51870, AT5G27520, and AT4G28390) are also induced.

Gluconeogenesis/Glyoxylate Cycle. Genes mediating steps of the gluconeogenesis/glyoxylate cycle, such as a pyruvate, orthodiphosphate dikinase (AT4G15530),

the glyoxysomal citrate synthases (AT3G58750 and AT2G42790; 2- to 5-fold), and Ala:glyoxylate aminotransferase (AT2G38400), are induced in the *im*W tissues (Eastmond and Graham, 2001).

In summary, relatively few genes involved in energy production show 2-fold or more differential regulation in *im*W tissues; fermentation is a notable exception where genes involved in all steps of this process are induced. Nevertheless, alterations in the expression of genes for key enzymes in the oxidative pentose-P pathway, the gluconeogenesis/glyoxylate cycle, and mitochondrial electron transport are consistent with the notion that both aerobic and anaerobic metabolism are up-regulated in *im*W, perhaps as a way to compensate energetically for a lack of photosynthesis in the white tissues.

Nitrogen Metabolism

The first step in nitrogen metabolism is reduction of nitrate, which is taken up by nitrate transporters. Transcription of a dual-affinity nitrate transporter (*NRT 1.1*) involved in both low- and high-affinity nitrate uptake is reduced in *im*W, while another nitrate transporter (*ATNRT2.6*), which has been shown to be insensitive to nitrate levels (Orsel et al., 2002; Chopin et al., 2007), is strongly induced in *im*W. Expression of two additional genes for key enzymes of nitrate assimilation, nitrite reductase (*NIR1*; 3-fold) and Gln synthetase (*GS2*; 3-fold), is strongly repressed in *im*W (Vincentz et al., 1993; Supplemental Table S1).

Consistent with the idea that *im*W sectors are perturbed in nitrogen metabolism, transcription from a large number of *im*W-responsive genes that mediate steps in amino acid biosynthesis is significantly altered. For example, *ATCYSD2*, *ATBCAT-3*, *ATBCAT-5*, AT3G02020, AT5G23010, AT4G23600, and AT1G15410 are repressed, while genes involved in Pro (*P5CS1*; 4.5-fold), Asn (*ASN1*; 124-fold), Glu (*GDH1* and *GDH2*; 2- and 13-fold, respectively), and branched-chain amino acid synthesis (*ATBCAT-2*; 30-fold) are induced. The induction of *ASN1* and *GDH1* has previously been shown to be a response to carbon limitation and to a change in the ratio of organic nitrogen to carbon in leaf tissues (Lam et al., 1996). Accompanying these changes, genes whose products are involved in protein and amino acid catabolism are generally induced in the *im*W tissues (Fig. 4; Supplemental Table S1). Examples include AT3G19390, AT3G10450, AT5G43580, AT2G45240, Pro oxidase, AT1G53580, and AT5G54080. Expression of several amino acid and oligopeptide transporters (*AAP1*, *AAT1*, *LHT7*, AT1G31820, AT2G 41190, AT1G22570, and AT4G21680; Fischer et al., 1998; Kerry et al., 2002) is also induced in *im*W tissues.

Taken together, these data support the notion that nitrogen metabolism is impaired in *im*W tissues and that this is accompanied by changes in amino acid metabolism, with a general decrease in amino acid biosynthesis and an increase in amino acid catabolism.

Sulfur Metabolism

Genes mediating the first two steps in sulfur assimilation, including ATP sulfurylase (*APS3*; 5-fold) and APS kinase (*AKN1*; 5-fold), are repressed in *im*W, suggesting a decrease in sulfur assimilation in *im*W tissues. These results correlate with the repression of genes involved in the synthesis of sulfur compounds in plants such as glucosinolates (AT5G23010, AT4G13770, and AT3G14210), Cys (AT3G13110, AT5G28020, AT2G43750, and AT3G59760), and nitrogen metabolism (Supplemental Table S1). The formation of Cys is a connecting step between sulfur and nitrogen assimilation in plants (Saito, 2004).

Lipid and Fatty Acid Metabolism

Very few genes involved in lipid and fatty acid metabolism are significantly altered in *im*W. In general, genes for phospholipid and galactolipid biosynthesis (AT4G29890, AT1G62430, AT1G73600, AT1G48600, and AT3G11670) are repressed, while those involved in lipid degradation, such as lipases (AT5G16120, AT5G14180, AT3G62590, etc.) and fatty acid β-oxidation family genes (*ACX1*, AT3G51840, AT3G06810, and AT4G14430), are induced in *im*W tissues. An exception to the general repression of lipid biosynthesis is the induction of a gene encoding an oleosin (AT5G56100). Oleosins are found on the surface of seed oil bodies and function as lipid storage reserves for the germinating seedlings (Ohlrogge and Jaworski, 1997). In contrast, genes mediating fatty acid biosynthesis and elongation are variably regulated in *im*W. For example, two AMP-binding proteins (AT5G16370 and AT5G27600), a peroxisomal CoA synthetase (AT3G48990), and a β-ketoacyl-CoA synthase family protein (AT2G28630; 2.7-fold) are induced, while other genes (β-hydroxyacyl-ACP dehydratase, *ACP2*, acyl-ACP thioesterase, and stearoyl-ACP desaturase) are repressed.

Although these alterations in lipid metabolism are complex, the data are consistent with the idea that lipid metabolism is impaired in *im*W tissues, with a decrease in lipid biosynthesis and an increase in lipid degradation, while fatty acid metabolism is variably regulated in these tissues.

Plant Defense and Stress Response

Consistent with the hypothesis that lack of carotenoids in *im*W leaf tissues results in photooxidative damage due to the production of ROS (Brown et al., 2001; Rodermel, 2001; Gray et al., 2002), the products of many *im*-responsive genes are involved in oxidative stress responses (Fig. 4; Supplemental Table S1). Some of the prominent examples include genes for proteins involved in the following.

General Oxidative Stress Response Genes, Which Are Largely Induced. For example, expression of copper-zinc superoxide dismutases (*CCS1* and *CSD2*; 3- and

5-fold, respectively), Fe-superoxide dismutase (*FSD3*; 2.3-fold), glutathione peroxidase (AT4G31870), ferritin 1 (*ATFER1*), heat shock protein 70 (*HSP70*), and a putative peroxidase (AT5G39580) is induced in *im*W, whereas transcription of a Fe-superoxide dismutase (*FSD1*; 2-fold) and catalase (*CAT3*) is repressed in *im*W tissues (Karpinski et al., 1993; Baier and Dietz, 2005).

Secondary Metabolism Genes, Which Are Largely Induced. These include genes involved in phenylpropanoid and flavonoid biosynthesis (*PAL1*, *PAL2*, *ATC4H*, *F3H*, *CCoAMT*, and *CAD*), cinnamoyl-CoA reductase (AT2G33590), and a flavonol synthase required for anthocyanin biosynthesis. Phenylpropanoids and flavonoids are frequently produced in response to biotic and abiotic stresses, including high light/UV, pathogen attack, wounding, and low temperature (Dixon and Paiva, 1995; Winkel-Shirley, 2002).

Ascorbate/Glutathione Cycle and Ascorbate Biosynthesis Genes, Some of Which Are Induced. These include a glutathione peroxidase (AT4G31870), stromal ascorbate peroxidase (*sAPX*; 2.5-fold), a glutathione reductase (AT3G24170), a glutathione peroxidase (AT2G31570), and *MIOX2* and *MIOX4* (Lorence et al., 2004). In contrast, genes for thylakoid ascorbate peroxidase (*tAPX*; 2.5-fold) and a putative dehydroascorbate reductase (*DHAR*; 3-fold) are repressed in *im*W.

Pro Biosynthesis and Catabolism Genes, Some of Which Are Induced in imW Tissues. These include Δ1-pyrroline 5-carboxylate synthase (*P5CS1*) and Pro oxidase (AT3G30775; 25-fold). Pro is known to function as an osmoprotectant and as a hydroxyl radical scavenger during water and salt stress conditions (Kiyosue et al., 1996).

Alternative Pathway of Electron Transport Genes, Some of Which Are Induced. As mentioned earlier, *AOX1A* and *AOX1D* are strongly induced in *im*W. *AOX1A* and *AOX1D* are known to be some of the most stress-responsive proteins among the mitochondrial proteins (Clifton et al., 2006).

Other Plant Defense and Stress-Related Response Genes, Which Are Variably Regulated. Genes for several other classes of plant defense and stress-related proteins, including those associated with heat, abscisic acid, cold, dehydration, Suc, and salt stress, are differentially regulated: some are induced while others are repressed (Supplemental Table S1; Cheong et al., 2002; Mahalingam et al., 2003).

Taken together, the differential regulation of a large number of plant defense and stress-related genes is remarkable and signifies that *im*W tissues are under stress, especially oxidative stress.

Transcript Profiling: *im*W versus NF-Treated White Tissues

Although we hypothesize that sink-source interactions play an important role in determining the molecular phenotype of *im*W sectors, the above data show that these interactions are likely integrated with oxidative and other stress responses that arise due to the nature of the primary lesion in *im* (i.e. photooxidation) due to a lack of colored carotenoids. Therefore, to gain further insight into the molecular phenotype of *im*W, we compared transcript profiles of NF-treated wild-type Arabidopsis leaves and *im*W leaves. Consistent with the idea that *im*W and NF-treated leaf tissues have a similar phenotype, previous studies demonstrated that both white tissues (1) have similar levels of *PDS* mRNA and protein, (2) accumulate phytoene due to inhibition of the PDS step of carotenogenesis, (3) have plastids with similar chloroplast ultrastructure, and (4) have decreased levels of nuclear mRNAs for various photosynthetic proteins (Reiß et al., 1983; Susek and Chory, 1992; Wetzel et al., 1994; Wetzel and Rodermel, 1998; Surpin et al., 2002). The white leaves from both tissue types are also anatomically similar: mesophyll cells are smaller and more numerous with fewer air spaces than normal, and the palisade cells fail to expand (Fig. 5A). In contrast to these striking similarities, there are also differences. For example, transcription of *Lhcb* (as monitored by an *Lhcb* promoter:GUS transgene) is significantly more down-regulated in NF-treated versus *im*W cells, suggesting that retrograde signaling might be different in the two tissue types (Meehan et al., 1996).

Previous global transcript profiling experiments of NF-treated Arabidopsis have been conducted with white cotyledon tissues from seedlings germinated in the presence of NF (Strand et al., 2003; Mochizuki et al., 2008; Moulin et al., 2008). However, in our studies, we used expanding white leaf tissues from 4-week-old plants sprayed with the herbicide (Fig. 5, A and B). We felt that this would provide a more compelling developmental context, since the *im*W sectors came from expanding *im* leaves (Fig. 5, A–C).

We first compared microarray data from NF-treated and wild-type samples. Like *im*W in Figure 1, the expression of many genes was similar to that in wild-type Arabidopsis green leaves, but 1,044 genes/probe sets were differentially regulated 2-fold or more in NF-treated white tissues versus the wild type (Supplemental Table S2). Of these, 721 genes were repressed and 323 genes were induced. We next performed cluster analysis of the 2-fold or more differentially regulated genes from the two white tissues (NF versus the wild type [1,044 genes] and *im*W versus the wild type [1,434 genes]) as a first approach to assess similarities and differences between *im*W and NF-treated tissues. This analysis resulted in six clusters (Supplemental Fig. S2; Supplemental Table S3). Many genes are regulated similarly in the *im*W and NF-treated tissues: in cluster 1, 759 genes from both tissues are repressed significantly compared with the wild type, while in cluster 3, 205 genes are induced significantly in both tissues. Clusters 2 and 4, on the other hand, define genes that are induced or repressed uniquely in *im*W versus the other two tissue types (728 genes), and clusters 5 and 6 define genes that are induced or repressed uniquely in the NF-treated tissues versus *im*W and wild-type tissues (179 genes). Interestingly,

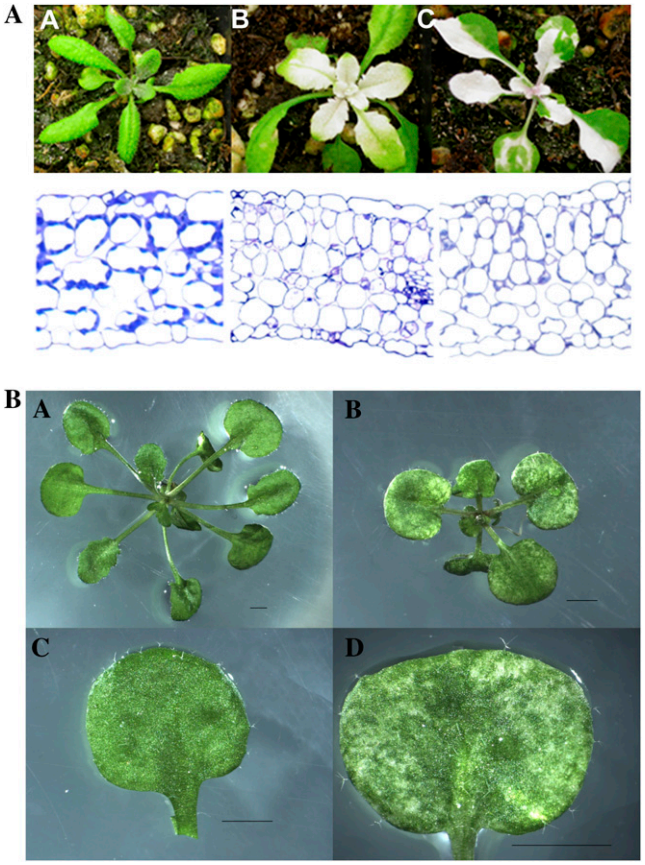

Figure 5. A, Anatomy of wild-type leaves and white sectors of *im* and NF-treated plants. All plants (top) were photographed at the same magnification (25×) 4 weeks after germination (22°C, 100 μmol m^{-2} s^{-1} continuous illumination). Light microscopy (bottom) was performed on cross sections of fixed, fully expanded leaves (as in Aluru et al., 2001). Image A, Wild-type Arabidopsis (Columbia). Image B, White leaf tissue from NF-treated wild-type Arabidopsis. Image C, White leaf sector from *im*. The mesophyll layers of the white tissues contain abnormal chloroplasts that do not stain as intensely as chloroplasts of wild-type leaves. B, Variegated phenotype of wild-type Arabidopsis plants treated with NF. Seeds from wild-type Arabidopsis plants were germinated and grown on Murashige and Skoog plates with or without NF for 3 weeks at 200 μmol m^{-2} s^{-1} continuous illumination. Image A, Wild type. Image B, Wild type with 0.025 μM NF. Image C, Individual leaf from A. Image D, Individual leaf from B. Bars = 2 mm.

not a single significant gene was induced in one white tissue and repressed in the other.

Functional classification of genes in cluster 2, the largest component of genes uniquely induced in *im*W versus NF-treated tissues, reveals that several different classes of genes are induced in *im*W (Supplemental Table S3, sheet 2). However, it is notable that many genes belonging to the plant defense, oxidative stress, and secondary metabolism groups are induced in *im*W versus NF-treated tissues (Table I). It is also interesting that the expression of several genes involved in plant development, including *DAG*, *CR88*, *DRM1*, *ATPSK4*, and *UNE6*, are induced only in *im*W. These genes play important roles in chloroplast biogenesis and in promoting germination, plant growth, flowering, and delayed senescence in Arabidopsis (Chatterjee et al., 1996; Cao et al., 2003; Pagnussat et al., 2005; Zhu et al., 2005; Matsubayashi et al., 2006). The *im*W-specific induction of these genes is consistent with the observation that Arabidopsis *im* develops normally and produces viable seeds, whereas NF-treated plants senesce and are not viable for long following treatment with NF (at the concentrations used in this study).

We next compared the *im*- and NF-responsive genes using the MapMan tool (Figs. 4 and 6). These studies revealed that, in general, the two tissue types have very similar expression profiles, especially with respect to the behavior of genes in pathways that were found to be markedly altered in *im*W versus the wild type (Fig. 4). These include (1) photosynthesis, photorespiration, Suc and starch metabolism, pigment biosynthesis, amino acid biosynthesis, and nitrate and sulfur assimilation, which are repressed in both tissues; (2) amino acid catabolism and ammonia assimilation, which are largely induced; and (3) other primary metabolic pathways, including glycolysis, fermentation, and TCA cycle, which are variably regulated in both white tissues.

Despite these similarities, our data show distinct differences between the two tissue types. A comparison of NF-treated (Fig. 6) versus *im*W (Fig. 4) tissues reveals that more genes for the Calvin cycle (11 versus five), photorespiration (six versus three), tetrapyrrole (five versus two) and amino acid (17 versus 12) biosynthesis, and nitrate (four versus three) and sulfur (four versus two) assimilation are repressed in the NF-treated versus *im*W tissues. In contrast, more genes for the ascorbate/glutathione cycle (four versus one), phenylpropanoid/flavonoid biosynthesis (11 versus three), and Suc (eight versus four) and amino acid (22 versus nine) catabolism are induced in *im*W versus NF-treated tissues. At the other extreme, our data show that mitochondrial electron transport is reciprocally regulated in these two white tissues. Genes for proteins such as NADH-ubiquinone oxidoreductase (complex I), ubiquinol-cytochrome *c* reductase (complex III), and AT3G46430 are repressed in NF-treated tissues, while other genes of the same pathway are induced in *im*W.

In summary, taking into consideration the large number of genes (Figs. 4 and 6) whose transcripts do not differ significantly in abundance, we conclude that the transcriptomes of *im*W and NF-treated tissues bear a striking resemblance, yet because there are differences, their molecular phenotypes are not identical.

One possibility to explain these differences is that they could be due to differences in the mechanism of inhibition of PDS in the two tissue types. As a first approach to test this hypothesis, we grew wild-type Arabidopsis plants on Murashige and Skoog medium with varying concentrations of NF. Interestingly, we observed variegation in wild-type Arabidopsis plants at NF concentrations ranging from 0.001 to 0.05 μM

Table I. *Expression data of a subset of genes in imG and imW leaf sectors and NF-treated white leaf tissues*

Fold change values of genes induced or repressed 2-fold or more ($P \leq 0.05$) in the three leaf tissues relative to the wild type are shown. Fold change values of less than 2 are considered unchanged (NC). The complete list of genes is provided in Supplemental Tables S1, S2, and S4.

Affymetrix Identifier	Locus Identifier	*im*G	*im*W	NF	Annotation
Photosynthesis					
254335_at	AT4G22260	−4.20	−4.60	NC	IM
258321_at	AT3G22840	5.56	NC	NC	ELIP1
245306_at	AT4G14690	4.26	5.96	6.79	ELIP2
251082_at	AT5G01530	NC	−2.10	NC	LHCB4
256015_at	AT1G19150	−2.50	−2.30	−3.275	LHCA6
258239_at	AT3G27690	−5.00	−19.50	−12.44	LHCB2:4
248151_at	AT5G54270	−2.50	−13.40	−8.32	LHCB3
258993_at	AT3G08940	−2.50	−6.95	−10	LHCB4.2
259491_at	AT1G15820	−2.50	−6.90	−9.53	LHCB6
264837_at	AT1G03600	−2.30	NC	NC	PSII family protein
263114_at	AT1G03130	−3.10	−5.95	−5.88	PSAD-2
265287_at	AT2G20260	−2.90	−6.38	−4.45	PSAE-2
254398_at	AT4G21280	−2.10	−2.81	−3.65	PSBQ
256979_at	AT3G21055	−2.20	−2.91	−11.28	PSBTN
244974_at	ATCG00700	−2.00	NC	NC	PSII low-molecular-weight protein
265735_at	AT2G01140	2.08	NC	NC	Fru-bisP aldolase
259749_at	AT1G71100	2.39	NC	NC	Rib-5-P isomerase
251762_at	AT3G55800	NC	−2.80	−4	SBPASE
265170_at	AT1G23730	8.23	NC	NC	Carbonic anhydrase
Suc/starch metabolism					
255016_at	AT4G10120	NC	−22.1	−38.91	SPS; Suc-P synthase
248687_at	AT5G48300	NC	−3.6	−5.33	ADG1; ADP-Glc pyrophosphorylase
245998_at	AT5G20830	NC	2.8	NC	SUS1; Suc synthase
263912_at	AT2G36390	NC	−3.2	−2.05	SBE2.1; starch-branching enzyme
249785_at	AT5G24300	NC	−2.0	−2.27	SSI; starch synthase
250007_at	AT5G18670	NC	2.9	2.21	BMY3; β-amylase
254101_at	AT4G25000	2.37	NC	NC	AMY1; α-amylase
245275_at	AT4G15210	4.46	−5.2	NC	β-Amylase
256787_at	AT3G13790	4.07	4.0	NC	ATBFRUCT1; cell wall invertase
256861_at	AT3G23920	2.07	4.0	NC	BMY7; β-amylase
258507_at	AT3G06500	NC	3.0	NC	Invertase
260969_at	AT1G12240	NC	2.8	NC	Vacuolar invertase
262038_at	AT1G35580	NC	2.6	3.01	CINV1; cytosolic invertase
264400_at	AT1G61800	8.07	15.4	NC	GPT2; Glc/phosphate transporter
257939_at	AT3G19930	2.09	NC	NC	STP4; sugar transporter
262456_at	AT1G11260	NC	3.3	3.21	STP1; sugar transporter
Glycolysis/TCA cycle					
260207_at	AT1G70730	NC	−2.3	−2.1	Phosphoglucomutase
247983_at	AT5G56630	NC	−2.2	NC	Phosphofructokinase
253987_at	AT4G26270	2.44	NC	NC	Phosphofructokinase family protein
247338_at	AT5G63680	2.17	NC	NC	Pyruvate kinase
248283_at	AT5G52920	−2.87	NC	NC	Pyruvate kinase
252300_at	AT3G49160	NC	5.47	4.91	Pyruvate kinase
245528_at	AT4G15530	3.06	3.09	3.07	Pyruvate orthodiphosphate dikinase
260590_at	AT1G53310	2.05	−2.6	NC	ATPPC1; PEP carboxylase
263491_at	AT2G42600	NC	−2.1	NC	ATPPC2; PEP carboxylase
250094_at	AT5G17380	NC	2.61	2.53	Pyruvate decarboxylase family protein
264953_at	AT1G77120	NC	11.32	NC	ADH1; alcohol dehydrogenase
263157_at	AT1G54100	3.47	10.33	NC	ALDH7B4; aldehyde dehydrogenase
248461_s_t	AT2G47510	−2.1	−3.3	−3.6	FUM1; fumarase
251541_at	AT3G58750	NC	2.40	2.32	CSY2; citrate synthase
263986_at	AT2G42790	2.75	2.55	NC	CSY3; citrate synthase
Mitochondrial electron transport					
245181_at	AT5G12420	5.56	2.69	NC	Unknown protein
250863_at	AT5G04750	2.00	NC	NC	F1F0-ATPase inhibitor protein
261317_at	AT1G53030	2.01	2.36	NC	Cytochrome *c* oxidase copper chaperone protein
257333_at	ATMG01360	2.39	NC	NC	Cytochrome *c* oxidase subunit 1

(*Table continues on following page.*)

Table I. (*Continued from previous page.*)

Affymetrix Identifier	Locus Identifier	*im*G	*im*W	NF	Annotation
255259_at	AT4G05020	2.64	NC	NC	NDB2; NAD(P)H dehydrogenase
266835_at	AT2G29990	2.74	NC	NC	NDA2; NADH dehydrogenase
260706_at	AT1G32350	15.51	13.30	NC	AOX1D; alternative oxidase
258452_at	AT3G22370	NC	2.13	NC	AOX1A; alternative oxidase
247060_at	AT5G66760	NC	2.29	NC	SDH1-1; succinate dehydrogenase
248049_at	AT5G56090	NC	3.03	NC	COX15; cytochrome oxidase
260536_at	AT2G43400	NC	2.56	NC	ETFQO; electron carrier
248162_at	AT5G54500	2.51	NC	NC	FQR1; flavodoxin-like quinine reductase
Nitrogen/sulfur metabolism					
249710_at	AT5G35630	NC	−2.65	−4.13	GS2; Gln synthetase
255558_at	AT4G01900	−2.47	−2.41	NC	GLB1; Gln synthetase B1
250100_at	AT5G16570	3.52	−5.72	NC	Gln synthetase 1;4
249581_at	AT5G37600	3.78	NC	NC	Gln synthase
265475_at	AT2G15620	NC	−3.06	−5.38	NIR1; nitrite reductase
245254_at	AT4G14680	NC	−4.22	−2.46	APS3; ATP sulfurylase 2
249112_at	AT5G43780	2.75	−2.01	NC	APS4; ATP sulfurylase 4
267112_at	AT2G14750	NC	−5.85	−6.17	APS kinase
252604_at	AT3G45060	NC	25.57	21.49	ATNRT2.6; nitrate transporter
264348_at	AT1G12110	NC	−8.17	−28.32	Nitrate transporter 1.1
245855_at	AT5G13550	2.24	NC	NC	SULTR4;1; sulfate transporter
Amino acid metabolism					
246701_at	AT5G28020	NC	−3.27	−31.62	ATCYSD2; Cys synthase
263696_at	AT1G31230	NC	−2.88	−4.32	AK-HSDH1 Asp kinase/homoserine dehydrogenase
257194_at	AT3G13110	NC	−2.82	−3.14	AtSerat2;2; Ser acetyltransferase
265305_at	AT2G20340	NC	−2.80	−2.1	Tyr decarboxylase
250385_at	AT5G11520	NC	2.38	NC	ASP3; Asp aminotransferase
264777_at	AT1G08630	NC	3.72	NC	THA1; Thr aldolase 1
252570_at	AT3G45300	NC	8.56	NC	IVD; isovaleryl dehydrogenase
250580_at	AT5G07440	2.20	13.40	NC	GDH2; Glu dehydrogenase
252415_at	AT3G47340	3.64	124.32	131.64	ASN1; Asn synthetase
250032_at	AT5G18170	NC	2.12	2.33	GDH1; Glu dehydrogenase
262177_at	AT1G74710	3.05	1.83	NC	ICS1; isochorisimate synthase
263539_at	AT2G24850	4.48	NC	NC	TAT3; Tyr aminotransferase
249527_at	AT5G38710	9.06	9.27	NC	Pro oxidase
251847_at	AT3G54640	2.29	NC	NC	TSA1; Trp synthase
253203_at	AT4G34710	2.34	NC	NC	ADC2; Arg decarboxylase
251775_s_t	AT2G39800	NC	4.47	4.09	P5CS1
Lipid metabolism					
261506_at	AT1G71697	2.18	NC	NC	ATCK1; choline kinase
259418_at	AT1G02390	3.24	NC	NC	ATGPAT2/GPAT2; acyltransferase
248050_at	AT5G56100	NC	2.68	NC	Gly-rich protein/oleosin
251143_at	AT5G01220	2.70	NC	NC	SQD2; sulfoquinovosyl diacylglycerol
258524_at	AT3G06810	2.28	3.76	NC	IBR3; acyl-CoA dehydrogenase/oxidoreductase
263432_at	AT2G22230	−2.50	−2.51	NC	β-Hydroxyacyl-ACP dehydratase, putative
263443_at	AT2G28630	NC	2.78	NC	β-Ketoacyl-CoA synthase family protein
266865_at	AT2G29980	−8.07	NC	NC	FAD3; fatty acid desaturase
267318_at	AT2G34770	−2.10	NC	NC	FAH1; fatty acid hydroxylase
261722_at	AT1G08510	NC	−2.54	−3.01	FATB; fatty acyl-ACP thioesterase
245249_at	AT4G16760	2.02	3.28	2.99	ACX1; acyl-CoA oxidase
249777_at	AT5G24210	2.07	NC	NC	Lipase class 3 family protein
251191_at	AT3G62590	3.20	3.00	NC	Lipase class 3 family protein
247717_at	AT5G59320	NC	6.24	2.31	LTP3; lipid transfer protein
247718_at	AT5G59310	NC	67.46	25.39	LTP4; lipid transfer protein
Secondary metabolism					
263845_at	AT2G37040	2.19	2.05	NC	PAL1; Phe ammonia-lyase
251984_at	AT3G53260	NC	2.39	NC	PAL2; Phe ammonia-lyase
250207_at	AT5G13930	2.22	NC	NC	ATCHS/CHS/TT4; chalcone synthase
253088_at	AT4G36220	4.47	NC	NC	FAH1; ferulate 5-hydroxylase
267470_at	AT2G30490	2.46	2.77	NC	C4H; trans-cinnamate 4-monooxygenase
252123_at	AT3G51240	6.49	3.42	2.25	F3H; naringenin 3-dioxygenase

(*Table continues on following page.*)

Table I. (*Continued from previous page.*)

Affymetrix Identifier	Locus Identifier	*im*G	*im*W	NF	Annotation
248200_at	AT5G54160	2.59	NC	NC	ATOMT1; *O*-methyltransferase 1
250738_at	AT5G05730	2.17	NC	NC	ASA1; anthranilate synthase
248185_at	AT5G54060	18.52	NC	NC	UDP-Glc:flavonoid 3-*O*-glucosyltransferase
249215_at	AT5G42800	15.69	NC	NC	DFR; dihydroflavonol reductase
260015_at	AT1G67980	8.09	14.44	NC	CCoAMT; caffeoyl-CoA *O*-methyltransferase
255787_at	AT2G33590	2.28	4.32	NC	Cinnamoyl-CoA reductase family
259911_at	AT1G72680	3.23	5.94	5.41	Cinnamyl-alcohol dehydrogenase
264514_at	AT1G09500	8.53	36.57	NC	Cinnamyl-alcohol dehydrogenase family
253277_at	AT4G34230	3.05	NC	NC	CAD5; cinnamyl-alcohol dehydrogenase
254283_s_t	AT4G22870	200.1	NC	NC	Anthocyanin synthase
245628_at	AT1G56650	8.97	NC	NC	PAP1; production of anthocyanin pigment
260140_at	AT1G66390	126.2	NC	NC	PAP2; production of anthocyanin pigment
Plant defense/stress					
255078_at	AT4G09010	−2.81	NC	NC	APX4; ascorbate peroxidase
252862_at	AT4G39830	4.87	NC	NC	L-Ascorbate oxidase
255142_at	AT4G08390	NC	2.359	NC	SAPX; L-ascorbate peroxidase
261149_s_t	AT1G19570	NC	−3.20	NC	DHAR1; dehydroascorbate reductase
258941_at	AT3G09940	5.73	NC	NC	MDHAR; monodehydroascorbate reductase
263426_at	AT2G31570	2.17	2.04	NC	ATGPX2; glutathione peroxidase
253496_at	AT4G31870	2.58	5.11	4.31	ATGXP7; glutathione peroxidase
257252_at	AT3G24170	2.64	2.37	NC	ATGR1; glutathione-disulfide reductase
253496_at	AT4G31870	2.58	5.109	4.31	ATGPX7; glutathione peroxidase
262119_s_t	AT1G02930	2.07	NC	NC	ATGSTF6; glutathione transferase
260405_at	AT1G69930	12.61	3.96	NC	ATGSTU11; glutathione transferase
253382_at	AT4G33040	2.60	NC	NC	Glutaredoxin family protein
259237_at	AT3G11630	−2.32	NC	NC	2-Cys peroxiredoxin
266385_at	AT2G14610	4.52	−5.23	−2.13	PR1; pathogenesis-related protein
258791_at	AT3G04720	2.23	NC	NC	PR4; pathogenesis-related
259925_at	AT1G75040	2.31	NC	NC	PR5; pathogenesis-related gene
250994_at	AT5G02490	2.44	NC	NC	HSP70-2; heat shock protein
245928_s_t	AT5G24770	2.56	NC	NC	VSP2; vegetative storage protein
251356_at	AT3G61060	2.59	3.52	NC	ATPP2-A13
265471_at	AT2G37130	9.76	NC	NC	Peroxidase 21
252291_s_t	AT3G49120	2.61	NC	NC	ATPCB/ATPERX34; peroxidase
246099_at	AT5G20230	4.06	5.90	4.72	ATBCB; blue copper ion binding
256012_at	AT1G19250	12.45	10.85	NC	FMO1; monooxygenase
259517_at	AT1G20630	NC	2.221	NC	CAT1; catalase
259544_at	AT1G20620	NC	−2.48	NC	CAT3; catalase
254098_at	AT4G25100	NC	−2.23	−71.33	FSD1; iron superoxide dismutase
249826_at	AT5G23310	NC	2.323	2.86	FSD3; iron superoxide dismutase
266165_at	AT2G28190	NC	3.454	2.59	CSD2; copper, zinc superoxide dismutase
256245_at	AT3G12580	NC	33.989	NC	HSP70 (heat shock protein 70); ATP binding
259511_at	AT1G12520	NC	5.128	3.38	CCS1; superoxide dismutase copper chaperone
Plant development					
245668_at	AT1G28330	NC	2.08	NC	DRM1; dormancy-associated protein
252234_at	AT3G49780	9.71	5.33	NC	ATPSK4; growth factor
263483_at	AT2G04030	NC	2.12	NC	CR88; embryo defective
246090_at	AT5G20520	NC	3.68	3.11	WAV2; wavy growth
255791_at	AT2G33430	NC	3.17	NC	Plastid developmental protein DAG, putative
246434_at	AT5G17520	−2.05	−2.4	−2.57	RCP1; root cap 1
259055_at	AT3G03340	NC	2.32	NC	UNE6; unfertilized embryo sac 6
247109_at	AT5G65870	3.99	NC	NC	ATPSK5; growth factor
251037_at	AT5G02100	2.82	NC	NC	UNE18; unfertilized embryo sac 18

(Fig. 5B). Below or above these concentrations, the plants were either visually wild type or albino, respectively. Moreover, the variegated plants appeared to be smaller in size than wild-type Arabidopsis plants grown on plates without NF. This is similar to our previous observations in Arabidopsis *im* plants, which are also smaller in size when compared with wild-type Arabidopsis plants (Aluru et al., 2001). These results suggest that the differences in the molecular phenotypes of the two white tissues may, in part, be due to

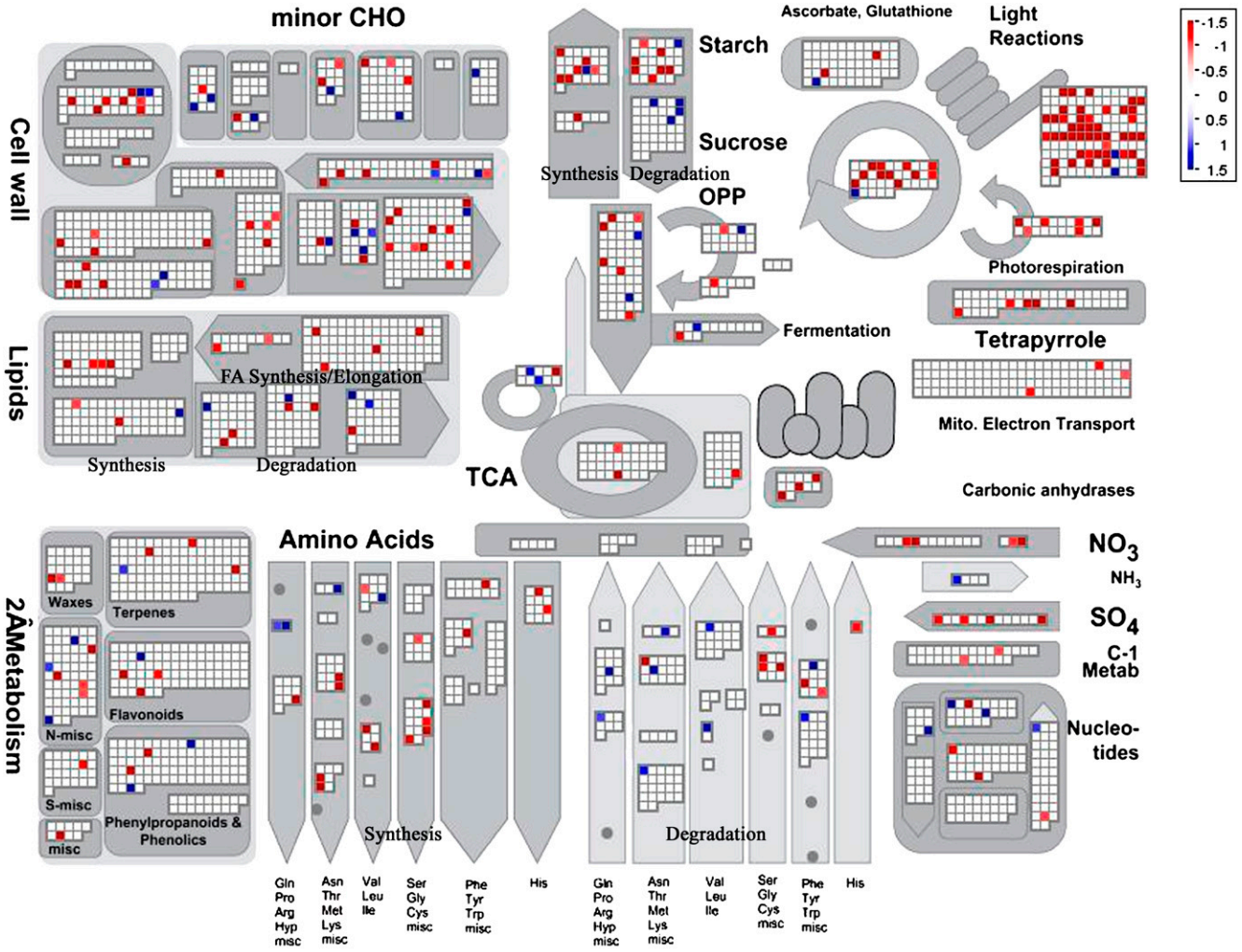

Figure 6. MapMan display of transcript profiling data. MapMan software (Thimm et al., 2004) was used to visualize changes in transcript abundance of the 2-fold or more differentially regulated genes associated with major metabolic pathways from NF white tissues. Induced genes are indicated in blue, and repressed genes are shown in red. White squares represent genes whose expression is unaltered versus the wild type. CHO, Carbohydrate.

the differential effects of PDS activity on chloroplast development and the nature of the mechanism of PDS inhibition in *im*W and NF-treated tissues.

Transcript Profiling: *im*W versus *im*G

Because both green and white sectors of *im* have the same genotype (i.e. *im*/*im*), we had previously hypothesized that *im*G sectors arise from cells that have avoided irreversible photooxidative damage, whereas white sectors form from cells that are photooxidized. Therefore, to further understand photooxidation in *im*W cells and the nature of compensating mechanisms that allow for the formation of *im*G, we compared the transcriptomes of *im*W and *im*G. Previous global transcript profiling studies have shown that 1,234 genes involved in various cellular processes are 3-fold or more differentially regulated in *im*G versus the wild type (Aluru et al., 2007). To make detailed comparisons between *im*W and *im*G, we first updated our previous data to include 2-fold or more differentially regulated genes from *im*G (versus the wild type). These analyses were performed as with *im*W and NF-treated tissues and show that 1,342 genes are 2-fold or more differential regulated in *im*G versus the wild type (Supplemental Table S4). We next compared the 2-fold or more differentially regulated genes from *im*G (1,342 genes) with those from *im*W (1,434 genes) by cluster analysis. This analysis resulted in seven different clusters and shows that there are many similarities and differences between the two tissue types (Supplemental Fig. S3; Supplemental Table S5). Approximately 780 genes are similarly regulated in *im*W and *im*G (58% of 1,342 genes from *im*G), while the rest are unique to one tissue or the other. Prominent examples of these similarities and differences in gene expression corresponding to major

metabolic pathways are listed in Table I and Supplemental Figure S4 and are discussed below.

Photosynthesis and Suc and Starch Metabolism

In contrast to *im*W, expression of genes for proteins mediating photosynthesis and Suc and starch metabolism is not significantly altered in *im*G. Exceptions to this include genes involved in the light reactions of photosynthesis (approximately 17 genes), which are repressed (Supplemental Table S4). Previous microarray analyses have shown that many of these genes, especially those involved in light harvesting, are down-regulated by high-light stress in Arabidopsis and are adaptations to avoid light stress (Kimura et al., 2003). Conversely, ELIP1, ELIP2, and a few genes of the Calvin cycle (AT4G14690, AT3G22840, AT2G01140, AT1G71100, and large subunit of Rubisco) are induced in *im*G. ELIP1 and ELIP2 are chlorophyll-binding proteins activated by high-light stress and are believed to be antistress proteins (Kimura et al., 2003), and genes involved in CO_2 fixation are induced during acclimation to high-light conditions (Hihara et al., 2001). The induction of the Calvin cycle genes is also consistent with previous reports from our laboratory showing an increase in photosynthetic carbon fixation in *im*G sectors (Aluru et al., 2007). Interestingly, expression of Suc and starch degradation genes such as BMY7, BFRUCT1, and STP4 is induced in both *im*W and *im*G. BFRUCT1 and STP4 are generally expressed in sink tissues. However, previous studies have shown that the expression of these genes is also induced in source tissues as a result of sink demand (Fotopoulos et al., 2003).

Glycolysis, TCA Cycle, and Mitochondrial Electron Transport

Genes for proteins mediating glycolysis (AT4G26270, AT5G63680, and AT1G53310) are induced in *im*G, while genes mediating fermentation, except those leading to the formation of acetate from pyruvate (AT1G54100), are not altered (Supplemental Table S4). Similar to *im*W, genes mediating mitochondrial electron transport are induced in *im*G. However, a number of additional genes involved in this pathway are induced only in *im*G (Table I; Supplemental Table S4). These results suggest that aerobic respiration, not fermentation, plays an important role in energy production in *im*G. The strong induction of mitochondrial electron transport genes is also necessary to provide a constant supply of extrachloroplastic ATP needed to maintain a sustained synthesis and export of Suc from "source" to sink tissues (Noctor et al., 2007).

Nitrogen and Sulfur Metabolism

Genes for proteins mediating nitrogen (AT5G16570 and AT5G37600) and sulfur (AT2G14750) metabolism and amino acid synthesis and degradation (e.g. AT1G74710, AT2G24850, AT5G38710, AT3G54640, and AT4G34710) are induced in *im*G. An increase in nitrogen supply to source tissues has been shown to enhance the gene expression and activities of many photosynthesis and sugar metabolism enzymes (Singletary et al., 1990; Martin et al., 2002).

Plant Defense and Oxidative Stress

It is noteworthy that several genes previously shown to be induced under high-light conditions are induced in *im*G (Table I; Supplemental Table S4). For example, genes mediating the ascorbate/glutathione cycle and genes for proteins involved in phenylpropanoid and flavonoid biosynthesis are significantly induced in *im*G. Although the expression of some of these genes is similar in both *im*W and *im*G, several more genes were significantly induced only in *im*G. In particular, genes involved in anthocyanin biosynthesis (AT4G22870, *PAP1*, and *PAP2*) are induced in *im*G; anthocyanin synthase and *PAP2*, a transcription factor mediating anthocyanin biosynthesis, are induced more than 100-fold. Anthocyanin synthesis has been shown to be increased under high-light conditions and helps to reduce light intensity within tissues (Rossel et al., 2002; Kimura et al., 2003). Furthermore, several other peroxidases and pathogenesis-related genes are uniquely induced in *im*G (Supplemental Table S4).

Taken together, these alterations in gene expression are consistent with our previous hypothesis that *im*G sectors act as source tissues for the white leaf sectors. In addition, the unique induction of a large number of ROS scavengers and other genes involved in dissipating absorbed light energy is indicative of the development of systems for high-light acclimation and/or adaptations to avoid light stress.

DISCUSSION

We had previously proposed that IM activity is particularly crucial during early chloroplast biogenesis when components of the photosynthetic apparatus are being synthesized and assembled on the thylakoid membrane. During this process, IM might serve as an alternative electron sink (a "safety valve") to regulate thylakoid membrane redox and prevent the generation of toxic oxygen radicals and photooxidation of the nascent photosynthetic apparatus (Aluru et al., 2006; Rosso et al., 2006). In *im*, we assume that some plastids are able to bypass the requirement for IM and form functional chloroplasts, which undergo division and sorting out to form clones of green cells (green sectors). However, other plastids are photooxidized early in development, and these also divide and give rise to clones of white plastids and cells by the process of sorting out. This results in white sectors.

Photooxidized tissues have been shown to have decreased expression of nuclear genes for many photosynthetic proteins (Reiß et al., 1983; Susek and Chory 1992; Wetzel et al., 1994; Wetzel and Rodermel, 1998;

Surpin et al., 2002). This, in turn, creates major metabolic sinks in white tissues and induces stress conditions, thus leading to the activation of different signaling mechanisms. Therefore, we hypothesize that there are multiple strategies and retrograde signals that integrate to bring about genome-wide changes in *im*W tissues. While we recognize that transcript accumulation is only one of a number of factors that regulate metabolism, the results from our studies provide compelling evidence that mRNA abundance might be a central regulatory factor in the response of some pathways to an inhibition of the PDS step of carotenogenesis. Figure 7 summarizes the metabolic adaptations, corresponding to major transcript changes, observed in *im*W leaf sectors. Not surprisingly, these strategies involve elements found in both sink and photooxidized tissues.

Nutrient Import into *im*W Leaf Sectors

Previous investigations in our laboratory demonstrated that the green leaf sectors of *im* have increased photosynthetic rates and Suc levels, whereas the white leaf sectors of *im* have low Suc levels and increased acid invertase activities, thus pointing toward the existence of a source-sink relationship between the two types of tissues (Aluru et al., 2001, 2007). In this study, global transcript profiling of *im*G sectors also reveals the induction of genes involved in major metabolic pathways (e.g. glycolysis, mitochondrial electron transport, nitrogen and sulfur metabolism, and amino acid biosynthesis); these alterations are typical of a "source" tissue (Singletary et al., 1990; Martin et al., 2002; Noctor et al., 2007). Conversely, our data show that photosynthesis genes are significantly repressed in *im*W, indicating a down-regulation of photosynthesis in *im*W tissues, without which there is very little or no de novo carbohydrate production (Figs. 4 and 7). The notion that carbohydrates are imported into the white tissues from *im*G sectors, probably as Suc, is substantiated by the strong induction of genes for invertases, fructokinases, and Suc synthase in addition to various sugar transporters, including a sugar transport protein (STP1; Caspari et al., 1994; Roitsch, 1999; Fig. 7). Invertases have been shown to influence resource allocation between source and sink tissues, and the induction of cell wall invertase and hexose transporters in the "sink" white tissues is perhaps needed to maintain the flow of Suc from source into the white tissues, where they would be hydrolyzed to Glc and Fru and further metabolized for growth and maintenance (Roitsch, 1999).

Concomitant with the repression of photosynthesis genes, some key nitrate and sulfur assimilatory genes are repressed in *im*W tissues (Figs. 4 and 7). These results are in agreement with previous reports demonstrating the down-regulation of genes/proteins of nitrogen and sulfur metabolism with a decrease in photosynthetic capacity (Masclaux et al., 2000; Deeken et al., 2006). These decreases are also accompanied by a repression of amino acid biosynthesis genes and by an induction of genes mediating amino acid degradation in *im*W. Therefore, we speculate that nitrogen sources, such as amino acids, are most likely obtained by white growing leaf tissues either by protein degradation or by import from the green sectors, perhaps in the form of Gln, Glu, and Asn, which are the chief nitrogen carriers in plants (Gilbert et al., 1998; Lam et al., 2003). This is supported by the induction of several genes mediating amino acid biosynthesis and transport (*AAT1*, *LHT1*, *LHT7*, *AAP1*, and *AAT1*) and oligopeptide transport (YSL1, YSL2, YSL3, and POT family transporters) in *im*G and *im*W and protein catabolism in *im*W tissues (Supplemental Tables S1 and S4; Fischer et al., 1998; Kerry et al., 2002). Moreover, the induction of Asn synthetase (*ASN1*) and Glu dehydrogenases (*GDH1* and *GDH2*) suggests that the nitrogen backbones released via catabolism of amino acids are reassimilated via Glu metabolism and transported as inertly stored Asn (Lam et al., 1996, 2003; Wong et al., 2004). Increased Pro synthesis (*P5CS* and Pro oxidase) could be a stress response, and Pro accumulation in response to stress is a widely reported phenomenon (Kiyosue et al., 1996).

Energy Production in *im*W Tissues

Our studies show that genes encoding proteins of complexes II and IV of the mitochondrial electron transport chain and mitochondrial metabolite transporters, including an ATP/ADP translocator, are induced in *im*W tissues, suggesting an increase in aerobic respiration (Figs. 4 and 7). Furthermore, the induction of Glu dehydrogenases (*GDH1* and *GDH2*) suggests that Glu metabolism plays an active role in mitochondrial oxygen consumption by providing intermediates for the TCA cycle and releasing NH_3^+ for reassimilation (Lam et al., 1996; Aubert et al., 2001).

The repression of genes for some of the proteins of glycolysis (phosphofructokinase and pyruvate kinase) and the TCA cycle (fumarase) suggests that these pathways might be down-regulated in *im*W (Figs. 4 and 7). This is in contrast to recent studies showing significant induction of glycolytic genes in Arabidopsis tumors, which represent sink tissues (Deeken et al., 2006). However, the fact that multiple enzymes are utilized by plants to catalyze essential steps of the glycolytic pathway (an inorganic pyrophosphate-dependent phosphofructokinase and phosphatase can also catalyze reactions catalyzed by the ATP-dependent phosphofructokinase and pyruvate kinase, respectively) and that intermediates for the TCA cycle are obtained from several different sources (e.g. the glyoxylate cycle and Glu metabolism) means that there is flexibility in maintaining flow through these pathways (Fernie et al., 2004). The strong induction of genes for all steps of the fermentation process (pyruvate decarboxylase and alcohol dehydrogenase), however, is striking and suggests that an up-regulation of this pathway is part of the strategy that *im*W tissues

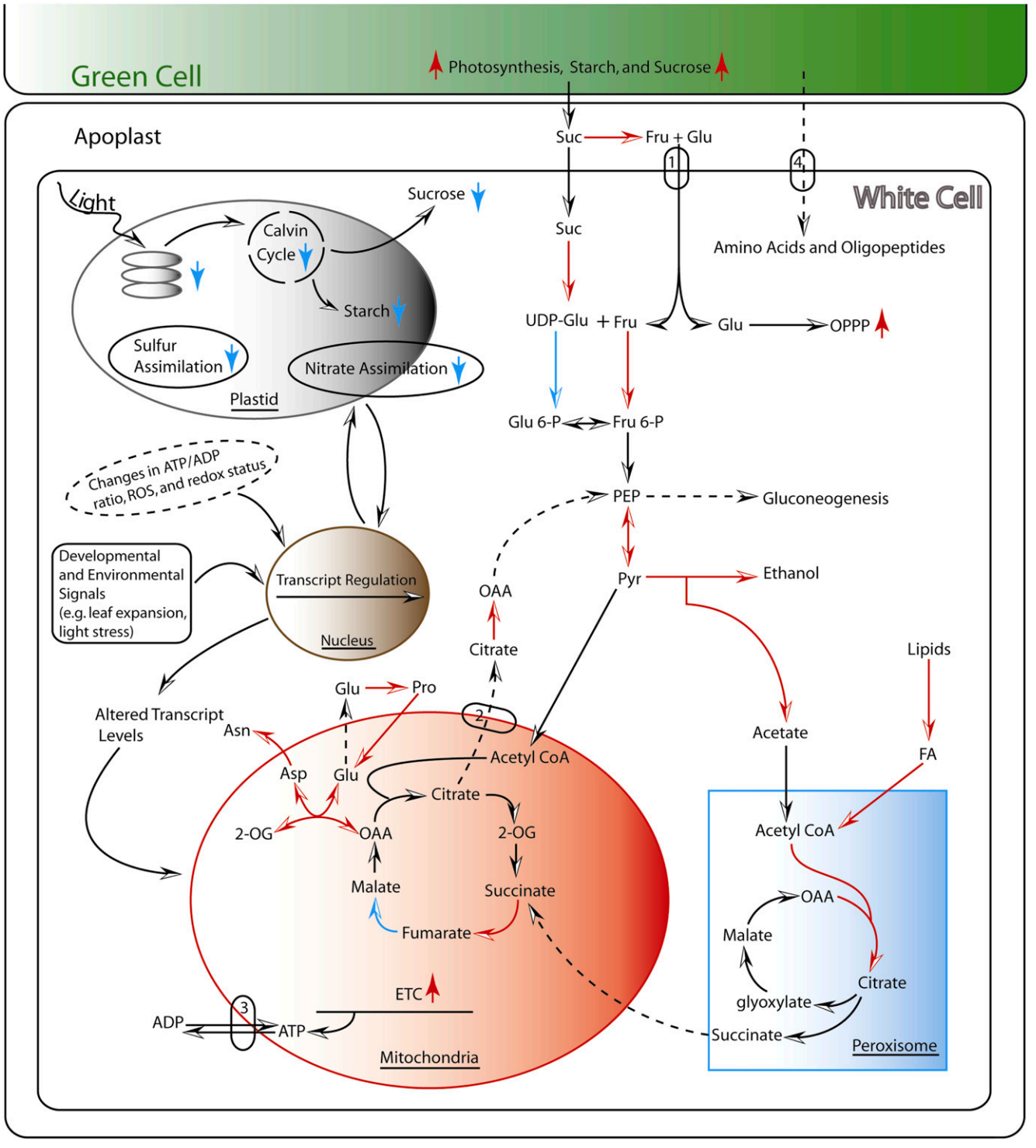

Figure 7. Schematic representation of the metabolic adaptations corresponding to major transcript changes in *im*W leaf sectors. See text for details. Red arrows indicate up-regulation, while blue arrows indicate down-regulation of metabolic pathways and/or steps in the metabolic pathway. Dashed lines represent hypothetical changes occurring in the *im*W tissues. Circles represent transporters: 1, sugar transporter; 2, metabolite transporter; 3, ATP/ADP translocator; 4, amino acid or oligopeptide transporter. ETC, Electron transport chain; OPPP, oxidative pentose-P pathway.

utilize to obtain energy (Fig. 7). These results are consistent with recent microarray data from Arabidopsis tumors, which were shown to have increased fermentation as well as mitochondrial respiration. An increase in fermentation activity in these tissues was attributed to a lack of intracellular air spaces in intact

tumors (Deeken et al., 2006). Figure 5A shows that cells in the white leaf tissues of *im* are smaller and contain fewer air spaces compared with green leaves of wild-type Arabidopsis. We conclude that lack of photosynthetic ATP production in the nongreen plastids of *im*W results in energy generation through the combined induction of both aerobic and anaerobic metabolism (Fig. 7).

It should be noted that fermentation may not only play a key role in ATP production in *im*W but may also provide acetate units for the glyoxylate cycle (Fig. 7). The repression of PEP carboxylases, which generate OAA from glycolytic intermediates, also suggests that the glyoxylate cycle may act to replenish the TCA cycle, especially under conditions in which two-carbon compounds such as acetate and ethanol are available for oxidative metabolism. In agreement with this, our data show induction of an aldehyde dehydrogenase and genes mediating fatty acid β-oxidation and the glyoxylate cycle (Figs. 4 and 7). Previous investigations have shown that acetate units generated from pyruvate by aldehyde dehydrogenase and/or from the breakdown of lipids by lipases and β-oxidation genes are utilized via the glyoxylate cycle to provide intermediates for the TCA cycle (Eastmond and Graham, 2001). In general, lipids are considered to be poor substrates for respiration in higher plants. However, as observed in some germinating seedlings, when the demand for carbon skeletons increases due to low concentrations of sugars, which is the case in *im*W sectors, the capacity to catabolize lipids may become crucial for the normal growth and development of Arabidopsis *im* (Eastmond et al., 2000).

Plant Defense and Stress Responses in *im*W Leaf Tissues

Our data show that there is an induction in *im*W of several oxidative stress genes, such as *CCS1*, *CSD2*, *FSD3*, *AOX1A*, and *AOX1D*, as well as of genes mediating steps in the ascorbate/glutathione cycle and in phenylpropanoid and flavonoid biosynthesis. Notable exceptions to these are *tAPX*, *FSD1*, and *CAT3*, which are repressed in *im*W tissues. Repression of *tAPX* could be due to the lack of proper thylakoid membrane structures in white plastids, whereas repression of *FSD1* and *CAT3* could be a response to the light environment (Redinbaugh et al., 1990; Kliebenstein et al., 1998). The *im*G sectors also show an induction of a whole battery of genes involved in oxidative stress protection as well as phenylpropanoid and flavonoid biosynthesis (Table I). One interesting observation is that many of these changes are common to both the green and white sectors of *im* (Aluru et al., 2007). One possible explanation for our data is that these alterations are first manifested during early chloroplast biogenesis in *im*G and white cells and that insufficient levels of photoprotective compounds during these stages result in some cells (white cells) being more susceptible to high-light conditions than others (green cells). This notion is further supported by the fact that the nonphotosynthetic pigments not only dissipate excess photon energy but also have antioxidant and ROS-scavenging activities that protect against oxidative stress (for review, see Edreva, 2005).

Several other plant defense and stress response genes were also observed to be differentially regulated in *im*W tissues (Supplemental Table S1). These include genes for proteins involved in heat, abscisic acid, cold, dehydration, Suc, and salt stresses as well as pathogen-related responses. A similar situation was observed in the barley mutant *albostrians*, where several stress- and pathogenesis-related genes were induced in the white leaf sectors versus the wild type (Hess et al., 1998). Although it is not clear, the differential regulation of many of these stress- and defense-related genes in *im*W could be a response to high light, the nutritional status of the white cell (e.g. low carbon), developmental processes, and/or the undifferentiated state of the white plastid, which could be interpreted by the white cell as multiple stress events, thus leading to the activation of different signal transduction pathways, as previously suggested by Hess et al. (1998).

im and NF-Treated White Leaves Have Overlapping But Distinct Transcriptomes

Although transcriptomics studies of NF-treated tissues lacking PDS activity exist, these studies were performed with different plant systems (4- to 6-d-old Arabidopsis seedlings) that consisted mainly of cotyledons and were also focused mostly on the analysis of specific metabolic pathways, not comprehensive analysis of the transcriptome (Strand et al., 2003; Mochizuki et al., 2008; Moulin et al., 2008). Because chloroplast development in cotyledons is different in many ways from that in true leaves (Shimada et al., 2007), we generated global gene expression data from NF-treated white leaf tissues to provide a valid comparison with our transcriptomics data from *im*W leaves.

Our data reveal that many genes in NF-treated tissues are regulated similar to the wild type. We also observed global responses to photooxidation in NF-treated and *im*W tissues at the levels of photosynthesis and carbohydrate, amino acid, nitrogen, and sulfur metabolism, indicating several similarities in the metabolic adaptations of these two tissue types (Figs. 4 and 6). Despite these general similarities, we found that 907 genes (48%) are differentially regulated in only one of the two tissue types. Many of these differences are *im* specific: cluster 2 shows that 602 genes are uniquely induced in *im*W versus NF-treated tissues (Supplemental Fig. S2). In particular, our data show that several genes involved in oxidative stress and plant development are uniquely induced in *im*W (Fig. 3; Supplemental Table S3, sheet 2). These changes are perhaps necessary for proper growth and development of the plant and for the formation of green cells during early chloroplast biogenesis.

While many of the primary metabolic pathways are similarly repressed in both tissue types (Figs. 4 and 6), more genes in a particular pathway are repressed in NF-treated tissues versus *im*W. One instance where this holds true involves the tetrapyrrole biosynthesis pathway. Two of the genes from the chlorophyll branch of the pathway (*PORB* and *PORC*) are repressed in *im*W, whereas five genes from the chlorophyll as well as the heme branches of the pathway are repressed in NF-treated tissues. Although our results are somewhat similar to recent reports from NF-treated tissues, those studies also demonstrated severe repression of several other genes of the tetrapyrrole biosynthesis pathway (Mochizuki et al., 2008; Moulin et al., 2008). One explanation could be that these studies were conducted using 4- to 6-d-old seedlings, not mature leaves, and that perhaps the tetrapyrrole biosynthesis genes are affected early in leaf development. Consistent with this notion, previous experiments have shown that expression of *HEMA1*, which catalyzes the rate-limiting step in the tetrapyrrole biosynthesis pathway, is less sensitive to NF treatment at later stages of plant development (McCormac and Terry, 2004). A striking difference is also found in the regulation of mitochondrial electron transport, which is reciprocally regulated in the two white tissues. In contrast, genes for fermentation (pyruvate decarboxylase) are induced in both tissue types (Figs. 4 and 6). These results suggest that perhaps NF-treated tissues gain energy mainly by anaerobic respiration via fermentation.

NF-Treated and *im*W Leaf Tissues: Why Are They Different?

One simple explanation for the differences between *im*W and NF-treated white tissues could be that genes respond to the same retrograde signal but with different sensitivities in the two white tissues. This may be particularly true in cases where a single gene is differentially regulated 2-fold or more in one white tissue and less than 2-fold but 1-fold or greater in another white tissue (Fig. 4; Supplemental Table S1). A second reason could be that the effect of a mutation in *im* was manifested early in plant development, whereas NF was applied much later in plant development. Thus, the developmental timing of PDS inhibition could be an important factor contributing to these differences. A third explanation could be due to the fact that *im*W sectors are randomly interspersed with the photosynthetically active green leaf sectors while NF-treated tissues are not. This could, perhaps, lead to differences in the source-sink interactions between the two tissue types. Therefore, we speculate that a comparison of *im*W tissues and white tissues from the variegated NF-treated leaf may show fewer differences in gene expression between the two white tissues than those shown in this study. Another reason could be the differences in the mechanism of PDS inhibition: while NF affects PDS activity, directly resulting only in phytoene accumulation, IM affects all reactions that transfer electrons into plastoquinone; thus, the redox status of the plastoquinone pool might be different in these two tissues. Plastoquinone is known to be a potent retrograde signaling molecule (Rodermel, 2001; Nott et al., 2006). Consistent with this idea, Figure 5B shows that the PDS activity, and hence the redox status of the plastoquinone pool, can be manipulated by changing the concentration of NF. Although the results from Figure 5B are similar to those previously observed with Arabidopsis *PDS* antisense and RNA interference mutants (Busch et al., 2002; Wang et al., 2005), to our knowledge, variegation in NF-treated tissues has not been reported previously. The results from Figure 5B also suggest that the mechanism of variegation in these mutants and NF-treated wild-type plants is similar to that in *im* and support our previous hypothesis that there is a threshold of electron capacity needed for phytoene desaturation to occur and green sectors to form (Wu et al., 1999). Below this threshold, carotenoids cannot be formed in sufficient quantity to prevent light-induced photooxidation and formation of the white sectors.

MATERIALS AND METHODS

Plant Material and Growth Conditions

Seeds from wild-type Arabidopsis (*Arabidopsis thaliana* ecotype Columbia) were surface sterilized and plated on Murashige and Skoog plates with or without the bleaching herbicide, NF. The seeds were subjected to a dark/cold treatment for 2 d at 4°C before incubating the plates at 150 μmol m^{-2} s^{-1} continuous illumination. Plants were grown with varying concentrations of NF (0.1, 0.05, 0.025, 0.01, and 0.005 μM) for 3 weeks before photographing. The experiment was repeated twice, and each experiment was conducted in duplicate to confirm leaf variegation.

For global transcript profiling studies, seeds from wild-type Arabidopsis (Columbia ecotype) and the *spotty* allele of *im* (Wetzel et al., 1994) were germinated and grown at 22°C under continuous illumination, first at 15 μmol m^{-2} s^{-1} for 5 d, then at 100 μmol m^{-2} s^{-1} for the rest of their growth. NF-treated seedlings were obtained by spraying 3-week-old wild-type seedlings once per day for 7 d with a 5 μM NF solution (Sigma-Aldrich). White sectors of NF-treated and *im* plants were dissected from leaves of prebolting-stage plants. Leaf tissues were frozen in liquid nitrogen and stored at –80°C until use.

RNA Isolation and Probe Preparation for Arabidopsis Oligoarrays

Total RNA was isolated from frozen tissue samples using the TRIzol reagent (GIBCO BRL). Three independent RNA preparations were made from pooled samples of each of the four tissue types (wild type, *im*W, *im*G, and NF white). Probes for Arabidopsis oligoarrays were made from 10 μg of total RNA following instructions in the Affymetrix GeneChip Expression Analysis Manual. The probes were then sent to the University of Iowa DNA Facility for hybridization, staining, and scanning of Affymetrix 22K ATH1 oligoarrays.

For quantitative real-time RT-PCR, first-strand cDNA was synthesized from DNase I-treated total RNA using the first-strand cDNA synthesis kit (Invitrogen). Real-time RT-PCR was then performed with the synthesized cDNAs according to the method given by Hewezi et al. (2008).

Microarray Data Analysis

Expression values were extracted from 12 ATH1 GeneChips (three replicates of each of the four tissue types: wild type, NF-treated white, *im*G, and *im*W) using the standard MAS 5.0 algorithm; implementation was provided by the R and Bioconductor packages (Gentleman et al., 2005). Default settings for MAS 5.0 were as suggested in the Bioconductor package. For normaliza-

tion, the microarray data were scaled to set the mean to 500, excluding 2% of the high-end and 2% of the low-end expression values based on intensity levels. Using the normalized data, average signal intensities were calculated from the three biological replicates of each tissue type. To avoid within-replicate variance, probe sets (genes) were chosen that had a coefficient of variation of 75% or less. For all results, a 5% significance level ($P \leq 0.05$) was assumed. Probe sets having a minimum 2-fold change in expression were used for functional analyses (differentially expressed genes).

Clusters were generated using the CLICK algorithm implemented in the EXPANDER package (Sharan et al., 2003). Expression values of differentially expressed genes were normalized using quantile normalization procedures and then standardized to mean 0 and variance 1 (methods provided by EXPANDER). Because NF2 (one of the biological replicates from the NF-treated tissues) showed high variability when compared with NF1 and NF3, it was excluded from the cluster analyses.

Differentially regulated genes were functionally classified using the Arabidopsis MIPS classification scheme and gene ontology searches (http://www.arabidopsis.org/). The MapMan (http://gabi.rzpd.de/projects/MapMan/) tool was used to group genes into metabolic pathways.

Light Microscopy

Samples for light microscopy were obtained from fully expanded leaves. Leaves from wild type, NF-treated, and *im* plants grown at 22°C under continuous illumination (100 μmol m^{-2} s^{-1}) were cut into 1-mm pieces, and light microscopy was performed as described by Aluru et al. (2001).

Supplemental Data

The following materials are available in the online version of this article.

Supplemental Figure S1. Scatterplot matrix of expression levels of all GeneChips.

Supplemental Figure S2. Cluster analysis of 2-fold differentially regulated genes from *im*W and NF-treated white tissues.

Supplemental Figure S3. Cluster analysis of 2-fold differentially regulated genes from *im*W and *im*G tissues.

Supplemental Figure S4. MapMan display of transcript profiling data.

Supplemental Table S1. The Affymetrix ATH1 oligoarray was used to determine gene expression differences between *im*W leaf sectors and wild-type (WT) Arabidopsis leaf tissues.

Supplemental Table S2. The Affymetrix ATH1 oligoarray was used to determine gene expression differences between NF-treated (NF) and wild-type (WT) Arabidopsis leaf tissues.

Supplemental Table S3. Categorization of different clusters from Supplemental Figure S2.

Supplemental Table S4. The Affymetrix ATH1 oligoarray was used to determine gene expression differences between *im*G and wild-type (WT) Arabidopsis leaf tissues.

Supplemental Table S5. Categorization of different clusters from Supplemental Figure S3.

Received January 16, 2009; accepted April 16, 2009; published April 22, 2009.

LITERATURE CITED

Aluru MR, Bae H, Wu D, Rodermel SR (2001) The Arabidopsis *immutans* mutation affects plastid differentiation and the morphogenesis of white and green sectors in variegated plants. Plant Physiol **127:** 67–77

Aluru MR, Stessman D, Spalding MH, Rodermel SR (2007) Alterations in photosynthesis in Arabidopsis lacking IMMUTANS, a chloroplast terminal oxidase. Photosynth Res **91:** 11–23

Aluru MR, Yu F, Rodermel S (2006) Arabidopsis variegation mutants: new insights into chloroplast biogenesis. J Exp Bot **57:** 1871–1881

Aubert S, Bligny R, Douce R, Gout E, Ratcliff R, Roberts J (2001) Contribution of glutamate dehydrogenase to mitochondrial glutamate metabolism studies by ^{13}C and ^{31}P nuclear magnetic resonance. J Exp Bot **52:** 37–45

Baier M, Dietz K (2005) Chloroplasts as a source and target of cellular redox regulation: a discussion on chloroplast redox signals in the context of plant physiology. J Exp Bot **56:** 1449–1462

Bolstad BM, Irizarray RA, Speed TP (2003) A comparison of normalization methods for high density oligonucleotide array data based on variance and bias. Bioinformatics **19:** 185–193

Brietenbach J, Zhu C, Sandmann G (2001) Bleaching herbicide norflurazon inhibits phytoene desaturase by competition with the cofactors. J Agric Food Chem **49:** 5270–5272

Brown EC, Somanchi A, Mayfield SP (2001) Interorganellar crosstalk: new perspectives on signaling from the chloroplast to the nucleus. Genome Biol **2:** 1021.1–1021.4

Busch M, Seuter A, Hain R (2002) Functional analyses of the early steps of carotenoid biosynthesis in tobacco. Plant Physiol **128:** 439–453

Cao D, Forehlich JE, Zhang H, Cheng C (2003) The chlorate resistant and photomorphogenesis-defective mutant cr88 encodes a chloroplast-targeted HSP90. Plant J **33:** 107–118

Carol P, Kuntz M (2001) A plastid terminal oxidase comes to light: implications for carotenoid biosynthesis and chlororespiration. Trends Plant Sci **6:** 31–36

Carol P, Stevenson D, Bisanz C, Breitenbach J, Sandmann G, Mache R, Coupland G, Kuntz M (1999) Mutations in the *Arabidopsis* gene IMMUTANS cause a variegated phenotype by inactivating a chloroplast terminal oxidase associated with phytoene desaturation. Plant Cell **11:** 57–68

Caspari T, Will A, Opekarova M, Sauer N, Tanner W (1994) Hexose/H^+ symporters in lower and higher plants. J Exp Biol **196:** 483–491

Chatterjee M, Sparvoli S, Edmunds C, Garosi P, Findlay K, Martin C (1996) DAG, a gene required for chloroplast differentiation and palisade development in Antirrhinum majus. EMBO J **15:** 4194–4207

Cheong YH, Chang H, Gupta R, Wang X, Zhu T, Luan S (2002) Transcriptional profiling reveals novel interactions between wounding, pathogen, abiotic stress, and hormonal responses in Arabidopsis. Plant Physiol **129:** 661–677

Chopin F, Orsel M, Dorbe M, Chardon F, Truong H, Miller AJ, Krapp A, Daniel-Vedele F (2007) The *Arabidopsis* ATNRT2.7 nitrate transporter controls nitrate content in seeds. Plant Cell **19:** 1590–1602

Clifton R, Millar AH, Whelan J (2006) Alternative oxidases in Arabidopsis: a comparative analysis of the differential expression in the gene family provides new insights into function of non-phosphorylating bypasses. Biochim Biophys Acta **1757:** 730–741

Cournac L, Redding K, Ravenel J, Rumeau D, Josse EM, Kuntz M, Peltier G (2000) Electron flow between photosystem II and oxygen in chloroplasts of photosystem-deficient algae is mediated by a quinol oxidase involved in chlororespiration. J Biol Chem **275:** 17256–17262

Dalla Vecchia F, Barbato R, La Rocca N, Moro I, Rascio N (2001) Responses to bleaching herbicides by leaf chloroplasts of maize plants grown at different temperatures. J Exp Bot **52:** 811–820

Deeken R, Engelmann JC, Efetova M, Czirjak T, Muller T, Kaiser WM, Tietz O, Krischke M, Mueller MJ, Palme K, et al (2006) An integrated view of gene expression and solute profiles of *Arabidopsis* tumors: a genome-wide approach. Plant Cell **18:** 3617–3634

Demmig-Adams B, Gilmore AM, Adams WW III (1996) In vivo functions of carotenoids in higher plants. FASEB J **10:** 403–412

Dixon RA, Paiva NL (1995) Stress-induced phenylpropanoid metabolism. Plant Cell **7:** 1085–1097

Eastmond P, Graham J (2001) Re-examination of the glyoxylate cycle in oil seeds. Trends Plant Sci **6:** 72–77

Eastmond PJ, Germain V, Lange PR, Bryce JH, Smith SM, Graham IA (2000) Postgerminative growth and lipid metabolism in oilseeds lacking the glyoxylate cycle. Proc Natl Acad Sci USA **97:** 5669–5674

Edreva A (2005) The importance of non-photosynthetic pigments and cinnamic acid derivatives in photoprotection. Agric Ecosyst Environ **106:** 135–146

Fernie AR, Carrari F, Sweetlove LJ (2004) Respiratory metabolism: glycolysis, the TCA cycle and the mitochondrial electron transport. Curr Opin Plant Biol **7:** 254–261

Fischer W, Andre B, Rentsch D, Krolkiewicz S, Tegeder M, Brietkreuz K, Frommer W (1998) Amino acid transport in plants. Trends Plant Sci **3:** 188–195

Fotopoulos V, Gilbert MJ, Pittman JK, Marvier AC, Buchanan AJ, Sauer

N, Hall JL, Williams LE (2003) The monosaccharide transporter gene, AtSTP4, and the cell wall invertase, Atßfruct1, are induced in Arabidopsis during infection with the fungal biotroph *Erysiphe cichoracearum*. Plant Physiol **132:** 821–829

Gentleman R, Carey V, Huber W, Irizarray R, Dudoit S (2005) Bioinformatics and Computational Biology Solutions Using R and Bioconductor. Springer-Verlag, New York

Gilbert GA, Gadush MV, Wilson C, Madore MA (1998) Amino acid accumulation in sink and source tissues of *Coleus blumei* Benth. during salinity stress. J Exp Bot **49:** 107–114

Gray JC, Sullivan JA, Wang J, Jerome CA, Maclean D (2002) Coordination of plastid and nuclear gene expression. Philos Trans R Soc Lond B Biol Sci **358:** 135–145

Hess W, Golz R, Borner T (1998) Analysis of randomly selected cDNA reveals the expression of stress- and defence-related genes in the barley mutant *albostrians*. Plant Sci **133:** 191–201

Hewezi T, Howe P, Maier TR, Hussey R, Mitchum MG, Davis E, Baum T (2008) Cellulose binding protein from the parasitic nematode *Heterodera schachtii* interacts with *Arabidopsis* pectin methyltransferase: cooperative cell wall modification during parasitism. Plant Cell **20:** 3080–3093

Hihara Y, Kamei A, Kanehisa M, Kaplan A, Ikeuchi M (2001) DNA microarray analysis of cyanobacterial gene expression during acclimation to high light. Plant Cell **13:** 793–806

Hirschberg J (2001) Carotenoid biosynthesis in flowering plants. Curr Opin Plant Biol **4:** 210–218

Howe CJ, Schlarb-Ridley BG, Wastl J, Purton S, Bendall DS (2006) The novel cytochrome c6 of chloroplasts: a case of evolutionary *bricolage*? J Exp Bot **57:** 13–22

Irizarray RA, Hobbs B, Collin F, Beazer-Barclay YD, Antonellis KJ, Scherf U, Speed TP (2003) Exploration, normalization and summaries of high density oligonucleotide array probe level data. Biostatistics **4:** 249–264

Joet T, Genty B, Josse EM, Kuntz M, Cournac L, Peltier G (2002) Involvement of a plastid terminal oxidase in plastoquinone oxidation as evidenced by expression of the Arabidopsis thaliana enzyme in tobacco. J Biol Chem **277:** 31623–31630

Josse EM, Simkin AJ, Gaffe J, Laboure AM, Kuntz M, Carol P (2000) A plastid terminal oxidase associated with carotenoid desaturation during chromoplast differentiation. Plant Physiol **123:** 1427–1436

Karpinski S, Wingsle G, Karpinska B, Hallgen J (1993) Molecular responses to photoxidative stress in *Pinus sylvestris* (L). II. Differential expression of Cu Zn-superoxide dismutases and glutathione reductase. Plant Physiol **103:** 1385–1391

Kerry K, Wiles AM, Sharp JS, Naider FR, Becker JM, Stacey G (2002) An oligopeptide transporter gene family in Arabidopsis. Plant Physiol **128:** 21–29

Kiyosue T, Yoshiba Y, Yamaguchi-Shinozaki K, Shinozaki K (1996) A nuclear gene encoding mitochondrial proline dehydrogenase, an enzyme involved in proline metabolism, is up-regulated by proline but down-regulated by dehydration in *Arabidopsis*. Plant Cell **8:** 1323–1335

Kimura M, Yamamoto YY, Seki M, Sakurai T, Sato M, Abe T, Yoshida S, Manabe K, Shinozaki K, Matsui M (2003) Identification of Arabidopsis genes regulated by high-light stress using cDNA microarray. Photochem Photobiol **77:** 226–233

Kliebenstein DJ, Monde R, Last R (1998) Superoxide dismutase in Arabidopsis: an eclectic enzyme family with disparate regulation and protein localization. Plant Physiol **118:** 637–650

Kruger N, von Schaewen A (2003) The oxidative pentose phosphate pathway: structure and organization. Curr Opin Plant Biol **6:** 236–246

Lam H, Wong P, Chan H, Yam K, Chen L, Chow C, Coruzzi GM (2003) Overexpression of the *ASN1* gene enhances nitrogen status in seeds of Arabidopsis. Plant Physiol **132:** 926–935

Lam HM, Coschigano KT, Oliveira IC, Melo-Oliveira R, Coruzzi GM (1996) The molecular-genetics of nitrogen assimilation into amino acids in higher plants. Annu Rev Plant Physiol Plant Mol Biol **47:** 569–593

Lorence A, Chevone B, Mendes P, Nessler C (2004) Myo-inositol oxygenase offers a possible entry point into plant ascorbate biosynthesis. Plant Physiol **134:** 1200–1205

Mahalingam R, Gomez-Buitrago A, Eckardt N, Shah N, Guevara-Garcia A, Day P, Raina R, Federoff NV (2003) Characterizing the stress/defense transcriptome of Arabidopsis. Genome Biol **4:** R20

Martin T, Oswald O, Graham IA (2002) Arabidopsis seedling growth, storage lipid mobilization, and photosynthetic gene expression are regulated by carbon:nitrogen availability. Plant Physiol **128:** 472–481

Masclaux C, Valadier M, Brugiere N, Morot-Gaudry J, Hirel B (2000) Characterization of the sink/source transition in tobacco (*Nicotiana tabacum* L) shoots in relation to nitrogen management and leaf senescence. Planta **211:** 510–518

Masuda T, Fusada N, Oosawa N, Takamatsu K, Yamamoto YY, Ohto M, Nakamura K, Goto K, Shibata D, Shirano Y, et al (2003) Functional analysis of isoforms of NADPH:protochlorophyllide oxidoreductase (POR), PORB and PORC, in Arabidopsis thaliana. Plant Cell Physiol **44:** 963–974

Matsubayashi Y, Ogawa M, Kihara H, Niwa M, Sakagami Y (2006) Disruption and overexpression of Arabidopsis phytosulfokine receptor gene affects cellular longevity and potential for growth. Plant Physiol **142:** 45–53

McCormac A, Terry M (2004) The nuclear genes *Lhcb* and *HEMA1* are differentially sensitive to plastid signals and suggest distinct roles for the GUN1 and GUN5 plastid signaling pathways during de-etiolation. Plant J **40:** 672–685

Meehan L, Harkins K, Chory J, Rodermel S (1996) Lhcb transcription is coordinated with cell size and chlorophyll accumulation (studies on fluorescence-activated, cell-sorter-purified single cells from wild-type and *immutans Arabidopsis thaliana*). Plant Physiol **112:** 953–963

Meskauskiene R, Nater M, Goslings D, Kessler F, op den Camp R, Apel K (2001) FLU: a negative regulator of chlorophyll biosynthesis in *Arabidopsis thaliana*. Proc Natl Acad Sci USA **98:** 12826–12831

Mochizuki N, Tanak R, Tanak A, Masuda T, Nagatani A (2008) The steady state level of Mg-protoporphyrin IX is not a determinant of plastid-to-nucleus signaling in Arabidopsis. Proc Natl Acad Sci USA **105:** 15184–15189

Moulin M, McCormac A, Terry M, Smith A (2008) Tetrapyrrole profiling in Arabidopsis seedlings reveals that retrograde plastid signaling is not due to Mg-protoporphyrin accumulation. Proc Natl Acad Sci USA **105:** 15178–15183

Noctor G, De Paepe R, Foyer CH (2007) Mitochondrial redox biology and homeostasis in plants. Trends Plant Sci **12:** 125–134

Nott A, Jung H, Koussevitzky S, Chory J (2006) Plastid-to-nucleus retrograde signaling. Annu Rev Plant Biol **57:** 739–759

Ohlrogge JB, Jaworski JG (1997) Regulation of fatty acid synthesis. Annu Rev Plant Physiol Plant Mol Biol **48:** 109–136

Orsel M, Filleur S, Fraisier V, Daniel-Vedele F (2002) Nitrate transport in plants: which gene and which control. J Exp Bot **53:** 825–833

Pagnussat GC, Yu H, Ngo QA, Rajani S, Mayalagu S, Johnson CS, Capron A, Xie F, Ye D, Sundaresan V (2005) Genetic and molecular identification of genes required for female gametophyte development and function in Arabidopsis. Development **132:** 603–614

Pego JV, Smeekens SCM (2000) Plant fructokinases: a sweet family get-together. Trends Plant Sci **5:** 531–536

Plaxton W (1996) The organization and regulation of plant glycolysis. Annu Rev Plant Physiol Plant Mol Biol **47:** 185–214

Redinbaugh MG, Sabre M, Sandalios JG (1990) Expression of the maize *Cat3* catalase gene is under the influence of a circadian rhythm. Proc Natl Acad Sci USA **87:** 6853–6857

Reiß T, Bergfeld R, Link G, Thien W, Mohr H (1983) Photoxidative destruction of chloroplasts and its consequences for cytosolic enzyme levels and plant development. Planta **159:** 518–528

Rodermel S (2001) Pathways of plastid-to-nucleus signaling. Trends Plant Sci **6:** 471–478

Roitsch T (1999) Source-sink regulation by sugar and stress. Curr Opin Plant Biol **2:** 198–206

Rossel JB, Wilson IW, Pogson BJ (2002) Global changes in gene expression in response to high light in Arabidopsis. Plant Physiol **130:** 1109–1120

Rosso D, Ivanov AG, Fu A, Geisler-Lee J, Hendrickson L, Geisler M, Stewart G, Krol M, Hurry V, Rodermel SR, et al (2006) IMMUTANS does not act as a safety valve in the protection of the photosynthetic apparatus of Arabidopsis during steady-state photosynthesis. Plant Physiol **142:** 574–585

Saito K (2004) Sulfur assimilatory metabolism: the long and smelling road. Plant Physiol **136:** 2443–2450

Sharan R, Maron-Katz A, Shamir R (2003) CLICK and EXPANDER: a system for clustering and visualizing gene expression data. Bioinformatics **19:** 1787–1799

Shimada H, Mochizuki M, Ogura K, Froehlich J, Osteryoung KW, Shirano Y, Shibata D, Masuda S, Mori K, Takamiya K (2007) *Arabi-*

dopsis cotyledon specific chloroplast biogenesis factor CYO1 is a protein disulfide isomerase. Plant Cell **19:** 3157–3169

Singletary GW, Doehlert DC, Wilson CM, Muhitch MJ, Below FE (1990) Response of enzymes and storage proteins of maize endosperm to nitrogen supply. Plant Physiol **94:** 858–864

Strand A, Asami T, Alonso J, Ecker JR, Chory J (2003) Chloroplast to nucleus communication triggered by accumulation of Mg-protoporphyrinIX. Nature **421:** 79–83

Sullivan JA, Gray JC (2002) Multiple plastid signals regulate the expression of the plastocyanin gene in pea and transgenic tobacco plants. Plant J **32:** 763–774

Surpin M, Larkin RM, Chory J (2002) Signal transduction between the chloroplasts and the nucleus. Plant Cell (Suppl) **14:** S327–S338

Susek RE, Chory J (1992) A tale of two genomes: role of chloroplast signal in coordinating nuclear and plastid genome expression. J Plant Physiol **19:** 387–399

Thimm O, Blaesing O, Gibon Y, Nagel A, Meyer S, Krüger P, Selbig J, Müller LA, Rhee SY, Stitt M (2004) MAPMAN: a user-driven tool to display genomics data sets onto diagrams of metabolic pathways and other biological processes. Plant J **37:** 914–939

Tonkyn JC, Deng X, Gruissem W (1992) Regulation of plastid gene expression during photooxidative stress. Plant Physiol **99:** 1406–1415

Vincentz M, Moureaux T, Leydecker MT, Vaucheret H, Caboche M (1993) Regulation of nitrate and nitrite reductase expression in Nicotiana plumbaginifolia leaves by nitrogen and carbon metabolites. Plant J **3:** 315–324

Wang T, Iyer LM, Pancholy R, Shi X, Hall TC (2005) Assessment of penetrance and expressivity of RNAi-mediated silencing of the *Arabidopsis phytoene desaturase* gene. New Phytol **167:** 751–760

Wetzel CM, Jiang CZ, Meehan LJ, Voytas DF, Rodermel SR (1994) Nuclear-organelle interactions: the immutans variegation mutant of Arabidopsis is plastid autonomous and impaired in carotenoid biosynthesis. Plant J **6:** 161–175

Wetzel CM, Rodermel SR (1998) Regulation of phytoene desaturase expression is independent of leaf pigment content in Arabidopsis thaliana. Plant Mol Biol **37:** 1045–1053

Winkel-Shirley B (2002) Biosynthesis of flavonoids and effects of stress. Curr Opin Plant Biol **5:** 218–223

Wong H, Chan H, Coruzzi GM, Lam H (2004) Correlation of *ASN2* gene expression with ammonium metabolism in Arabidopsis. Plant Physiol **134:** 332–338

Wu D, Wright DA, Wetzel C, Voytas DF, Rodermel SR (1999) The *immutans* variegation locus of *Arabidopsis* defines a mitochondrial alternative oxidase homolog that functions during early chloroplast biogenesis. Plant Cell **11:** 43–55

Yu F, Fu A, Aluru M, Park S, Xu Y, Liu H, Liu X, Foudree A, Nambogga M, Rodermel S (2007) Variegation mutants and mechanisms of chloroplast biogenesis. Plant Cell Environ **30:** 350–365

Zhu Y, Zhao H, Ren GD, Yu XF, Cao SQ, Kuai BK (2005) Characterization of a novel developmentally retarded mutant (drm1) associated with the autonomous flowering pathway in Arabidopsis. Cell Res **15:** 133–140